Accepted Manuscript

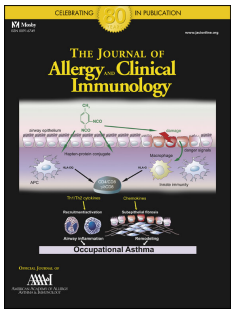

Aeroallergen-induced IL-33 predisposes to respiratory virus-induced asthma by dampening anti-viral immunity

Jason P. Lynch, PhD, Rhiannon B. Werder, BSc (Hons), Jennifer Simpson, B Biomed Sci (Hons), Zhixuan Loh, B Biomed Sci (Hons), Vivian Zhang, PhD, Ashraful Haque, PhD, Kirsten Spann, PhD, Peter D. Sly, MD, PhD, Stuart B. Mazzone, PhD, John W. Upham, MD, PhD, Simon Phipps, PhD

PII: S0091-6749(16)30150-6

DOI: 10.1016/j.jaci.2016.02.039

Reference: YMAI 12066

To appear in: *Journal of Allergy and Clinical Immunology*

Received Date: 10 July 2015

Revised Date: 25 January 2016

Accepted Date: 9 February 2016

Please cite this article as: Lynch JP, Werder RB, Simpson J, Loh Z, Zhang V, Haque A, Spann K, Sly PD, Mazzone SB, Upham JW, Phipps S, Aeroallergen-induced IL-33 predisposes to respiratory virus-induced asthma by dampening anti-viral immunity, *Journal of Allergy and Clinical Immunology* (2016), doi: 10.1016/j.jaci.2016.02.039.

Aeroallergen-induced IL-33 predisposes to respiratory virus-induced asthma by dampening anti-viral immunity

Jason P. Lynch, PhD,[1*], Rhiannon B. Werder, BSc (Hons),[1*], Jennifer Simpson, B Biomed Sci (Hons),[1], Zhixuan Loh, B Biomed Sci (Hons),[1], Vivian Zhang, PhD,[1], Ashraful Haque, PhD,[2], Kirsten Spann, PhD,[3,4], Peter D. Sly, MD, PhD,[4,5], Stuart B. Mazzone, PhD,[1], John W. Upham, MD, PhD,[4,6,], and Simon Phipps, PhD,[1,4]

[1]School of Biomedical Sciences, University of Queensland, Queensland 4072, Australia;

[2]QIMR Berghofer Medical Institute, Queensland 4006, Australia

[3]School of Biomedical Sciences, Queensland University of Technology, Queensland 4029, Australia;

[4]Australian Infectious Diseases Research Centre, The University of Queensland, Queensland 4072, Australia;

[5]Queensland Children's Medical Research Institute, The University of Queensland, Queensland 4006, Australia;

[6]Lung and Allergy Research Centre, School of Medicine, The University of Queensland, Princess Alexandra Hospital, Brisbane, Queensland 4102, Australia;

* The authors contributed equally.

Correspondence and reprints:

Dr. Simon Phipps, School of Biomedical Sciences, The University of Queensland, St. Lucia, Queensland 4072, Australia

s.phipps@uq.edu.au

phone 61(0)733652785

fax 61(0) 7 33651766

The authors have no conflicting financial interest. This work was supported by an equipment grant (Rebecca L. Cooper Medical Research Foundation), an ARC Future Fellowship to S.P. and an Australian Infectious Disease Research Excellence Award.

Abstract

Background. Frequent viral lower respiratory infections in early-life are an independent risk factor for asthma onset. This risk, and the development of persistent asthma, is significantly greater in children who later become sensitized.

Objective. To elucidate the pathogenic processes that underlie the synergistic interplay between allergen exposures and viral infections.

Methods. Mice were inoculated with a murine-specific Pneumovirus (Pneumonia virus of mice; PVM) and exposed to low-dose cockroach extract (CRE) in early- and later-life, and airway inflammation, remodeling and hyperreactivity assessed. Mice were treated with anti-IL-33 or apyrase to neutralize or block the release of IL-33.

Results. PVM infection or CRE exposure alone failed to induce disease whereas PVM/CRE co-exposure acted synergistically to induce the hallmark features of asthma. CRE exposure during virus infection in early-life induced a biphasic IL-33 response and impaired IFN-α and IFN–λ production, which in turn increased epithelial viral burden, airway smooth muscle growth, and type-2 inflammation. These features were ameliorated when CRE-induced IL-33 release was blocked or neutralized, while substitution of CRE with exogenous IL-33 recapitulated the phenotype observed in PVM/CRE co-exposed mice. Mechanistically, IL-33 down-regulated viperin and IFN regulatory factor 7 gene expression, and rapidly degraded IRAK1 expression in pDC both *in vivo* and *in vitro*, leading to TLR7 hypo-responsiveness and impaired IFN-α production.

Conclusion. We identify a hitherto unrecognized function of IL-33 as a potent suppressor of innate antiviral immunity, and demonstrate that IL-33 contributes significantly to the synergistic interplay between respiratory virus and allergen exposures in the onset and progression of asthma.

Key messages:

- Aeroallergen-induced IL-33 release suppresses antiviral immunity, increasing the severity of viral bronchiolitis.
- IL-33 impairs antiviral immunity by degrading IRAK1 and viperin in pDCs leading to a state of TLR7 hypo-responsiveness.
- Co-exposure to virus and allergen in early-life predisposes towards asthma progression in later-life.

Capsule summary:

Aeroallergen exposure perturbs the host response to Pneumovirus infection in early-life and predisposes toward virus/allergen provoked asthma. Aeroallergen-induced IL-33 dampens virus-induced IFN production by degrading IRAK1 and viperin in pDC to establish a microenvironment that is conducive for the expansion of type-2 inflammation.

Key words:

pneumonia virus of mice, IL-33, type-2 innate lymphoid cell, antiviral, respiratory syncytial virus, interferon, plasmacytoid dendritic cell

Abbreviations:

AEC: Airway epithelial cell
ASM: Airway smooth muscle
BALF: Bronchoalveolar lavage fluid
CRE: Cockroach extract
HDM: House dust mite
IFN: Interferon
IL: Interleukin
ILC2: Type-2 innate lymphoid cell
IRAK: Interleukin-1 receptor associated kinase 1
ISG: Interferon stimulated gene
pDC: Plasmacytoid dendritic cell
PVM: Pneumonia virus of mice
RSV: Respiratory syncytial virus
TLR: Toll-like receptor

vLRI: Viral lower respiratory tract infection

Introduction

Pathologically, asthma is characterized by airway inflammation and airway remodeling; structural changes including goblet cell metaplasia, increased deposition of extracellular matrix proteins, and increased airway smooth muscle (ASM) mass. These features collectively contribute to airway narrowing, loss in lung function, and airway hyperreactivity (AHR), and are poorly responsive to conventional therapies[1, 2]. The inflammatory response is typically of a type-2 cytokine profile, which promotes the recruitment and survival of key effector cells such as eosinophils and mast cells, and can induce features of airway remodeling through direct activation of airway epithelial and mesenchymal cells[3, 4]. Both CD4+ T helper 2 (Th2) cells and type-2 innate lymphoid cells (ILCs) produce the type-2 cytokines IL-5 and IL-13[5] in response to the tissue alarmin IL-33, and work collaboratively to affect their teleological role, namely anti-helminthic immunity[6]. However, why type-2 immunity is elevated during acute exacerbations of asthma, most commonly triggered by a respiratory virus infection, remains less clear.

Epidemiological studies have reproducibly demonstrated that severe/frequent viral lower respiratory tract infections (vLRI) in early-life are a major independent risk factor for asthma inception[7-9]. Notably, this association is markedly increased in children who later become sensitized to food or aeroallergens, and significantly, confers the greatest risk for progression to severe and/or persistent asthma[10-12]. The underlying mechanisms remain poorly defined, although it is likely that the synergistic interaction between allergen exposures and respiratory virus infection is underpinned by genetic and/or functional defect(s) in a shared antiviral immune pathway necessary for viral control in early-life[11]. Phenotypically this may manifest as a deficiency in the production of the antiviral cytokines, IFN-α, IFN-β and IFN-λ, by leukocytes and airway epithelial cells (AECs)[13-15], although whether such defects are virus-specific, genetic or acquired, for example as a consequence of a type-2 inflammatory milieu, remains highly contentious[16-18].

Plasmacytoid dendritic cells (pDC) are amongst the first cells to respond to a viral infection; sensing viral RNA and producing vast amounts of IFN-α/β downstream of toll-like receptor (TLR)7 activation[19, 20]. Defects in pDC and TLR7 responsiveness are associated with bronchiolitis, infant wheeze, and childhood asthma[21, 22]. In recent studies, we have used the natural mouse pathogen pneumonia virus of mice (PVM), which unlike human RSV, replicates more readily in mice to induce the more severe symptoms of infantile RSV bronchiolitis[20, 23]. TLR7 gene-deletion delayed the antiviral response, causing a severe viral bronchiolitis and the release of the alarmin IL-33 in early-life, and consequently, an asthma-like pathology developed upon viral challenge in later-life[20, 24]. Of note, the transfer of TLR7-sufficient, but not deficient pDC, ameliorated bronchiolitis, suggesting that perturbations to the pDC compartment in early-life predispose to AEC damage and IL-33 release, and hence may underlie the association between severe vLRI and the onset of asthma[21]. Intriguingly, IL-33 and its receptor, IL-1 receptor-like 1 (IL1RL1, also known as ST2), are susceptibility loci for wheezing in infancy (and asthma)[25, 26], although the molecular basis for this association is not known. This led us to question whether allergen-induced release of IL-33 increases the severity of virus-induced bronchiolitis by dampening pDC-orchestrated innate antiviral immunity, and to assess whether this early-life interaction causes persistent changes to host immunity that underlie disease progression in response to viral and/or allergen challenge in later-life.

METHODS

Experimental Procedures

Detailed description of materials and procedures is provided in the Methods section in this article's Online Repository at www.jacionline.org.

Induction of co-virus and allergen-induced asthma and associated perturbations.

Specific pathogen-free BALB/c mice or 4C13R mice [27] were inoculated with PVM (strain J3666; 1 pfu 'early life'; 20 pfu 'later life') or cockroach allergen extract (CRE, 1 µg) as previously described [20, 28] and as outlined in the study design (Figure 1A). In some experiments, mice were exposed to HDM extract (5 µg or 100ug), LPS (186 pg), recombinant IL-33 (10 ng), anti-IL-33/isotype control antibody (200 µg), apyrase (4 U/mL) or pyridoxalphosphate-6-azophenyl-2',4'-disulfonic acid (PPADS, 100 µm in 10uL). All studies were approved by The University of Queensland Animal Ethics Committee. Sample processing is described in the Methods section in this article's Online Repository.

Flow cytometry

Lungs were digested to single cell suspensions as previously described[24] then incubated with anti-FcγRIII/II before incubation with fluorochrome-conjugated antibodies at 4°C for 30 minutes, as described in the Methods section in this article's Online Repository.

Histology and Immunohistochemistry

Paraffin-embedded lung sections were prepared as described[20] then stained with Chromotrope 2R, Periodic acid-Schiff, Masson's Trichrome**,** anti-IL-33, anti-PVM G protein, anti-α-SM actin or anti-periostin as described in the Methods section in this article's Online Repository.

Measurement of protein expression

IL-33, IFN-λ2/3, IL-12p40, IFN-γ, IL-13, IL-5 were quantified by ELISA. IFN-α and IL-13 were quantified by CBA. IgG1a was detected using an in-house ELISA system[28].

Quantitative real time PCR

Total RNA was isolated with TriReagent solution followed by phenol-chloroform extraction. Reverse transcription was performed using M-MLV reverse transcriptase and random primers. qRT-PCR was performed with SYBR Green using the primers described in Table S1.

Airway function assessment

Airways resistance was determined by forced oscillation technique in response to methacholine, as previously described[29].

Type-2 innate lymphoid cell culture

Type 2 ILCs were FACS-sorted from PVM/CRE co-exposed mice at 10 dpi. Cells were cultured with IL-2 (30 ng/mL) and pre-incubated with IFN-α (5000U/mL) before stimulation with IL-33 (30 ng/mL).

Plasmacytoid dendritic cell culture

Bone marrow-derived pDC were generated as described previously[20]. pDC were pre-incubated with IL-33 (3 ng/mL) then stimulated with imiquimod (3 µg/mL).

Statistical analyses

Data were analyzed using a Student's t-test, one-way ANOVA with a Tukey post-hoc test or two-way ANOVA with a Sidak post-hoc test, as appropriate, using GraphPad Prism software (version 5.0; GraphPad Software, La Jolla, Calif). A P value <0.05 was considered statistically significant.

Results

Pneumovirus and allergen co-exposure synergise to promote asthma onset and progression

To interrogate the synergistic interaction between a respiratory virus infection and allergen exposures, we first identified a dose of cockroach extract (CRE) that by itself would not induce allergic inflammation. As we had previously developed a mouse model of virus-induced asthma by inoculating mice with PVM at 7 and 49 days of age[24], we elected to expose mice to CRE (i.n. route) at 10 days of age (i.e. 3 days after the primary virus inoculation; 'early-life'), followed by a series of CRE exposures (challenges in 'later-life') at 52, 59, 66, and 73 days of age (i.e. starting 3 days after virus challenge; see study design in Fig 1A). Repeated exposure to 10 or 100 μg, but not 0.1 or 1 μg of CRE (in the absence of PVM infection), induced peribronchial eosinophilia and mucous hypersecretion (Fig E1 in online repository). Therefore, we elected to use 1 μg of CRE for all further studies. To assess for a synergistic effect between PVM and CRE, we superimposed a low-dose PVM infection, which by itself did not induce features of type-2 inflammation (Fig 1B-D, Fig 2 in online repository), onto the low-dose CRE exposure model (Fig 1A). Eosinophilic inflammation, mucous hypersecretion, CRE-specific IgG1a (Fig 1B-D) and mucosal mast cells (data not shown) were greatest in mice exposed to both PVM and CRE. By contrast, these features of type-2 inflammation were absent in mice exposed to PVM alone or low dose CRE alone in both early and later-life, or low dose CRE alone in later-life (Fig 1B-D, Fig E2 in online repository). Similarly, features of airway remodeling including collagen and periostin deposition, and airway smooth muscle (ASM) remodeling (Fig 1E-G) were only evident in PVM/CRE co-exposed mice. To compare our findings to contemporary acute models of allergen-induced disease[30], we exposed a group of mice to high dose (100 μg) CRE in later-life alone. Strikingly, this regimen elicited type-2 inflammation, but was not sufficient to elicit features of airway remodeling (Fig E2 in online repository). Thus, low dose virus and low dose allergen co-exposures acted synergistically to induce all of the cardinal features of asthma.

Virus and allergen exposure in early- and later-life are necessary for maximal asthma severity.

We next addressed the relative contribution of the virus and allergen exposures in early- and later-life. PVM/CRE co-exposure in early-life alone was not sufficient to induce type-2 inflammation or airway remodeling as compared to the vehicle treated group (Fig E2 in online repository). The importance of both the virus and allergen challenge for asthma progression was confirmed when the omission of either exposure significantly diminished airway inflammation, airway remodeling, and AHR when assessed at 76 days of age (Fig E2 in online repository). These findings led us to question the importance of the CRE exposure during primary virus infection. Remarkably, when this exposure was omitted, type-2 inflammation, airway remodeling, and AHR were completely absent (Fig 1, final row), even though the mice had been infected with PVM in early and later-life, then challenged repeatedly with CRE. Taken together, these data suggested that the CRE exposure in early-life fundamentally altered the nature of the host response to secondary virus and/or allergen exposure in later-life, and that this effect was necessary for disease progression.

Allergen exposure increases viral load and lung tissue damage, and dampens antiviral cytokine production

Aeroallergens are known to rapidly induce innate inflammation in the airways[28, 31, 32]. We hypothesised that allergen-induced inflammation may perturb the host's antiviral response to PVM, thus increasing the severity of viral bronchiolitis. Viral load in the airway epithelium was significantly greater and persisted for longer in PVM/CRE co-exposed mice compared to mice inoculated with virus alone (Fig 2A and Fig E3A in online repository). In children with severe RSV bronchiolitis, the virus can spread to the parenchyma[33], however, few PVM-immunoreactive cells were observed in the alveoli (data not shown). Strikingly, PVM/CRE co-exposure stunted weight gain and heightened tissue oedema, indicative of severe disease (Fig 2B-C). The elevated viral illness in PVM/CRE co-exposed mice was associated with significantly lower IFN–α, IFN-λ and IL-12p40 but not IFN–γ production in the bronchoalveolar fluid (BALF) (Fig 2D), and attenuated

transcription of interferon stimulated genes (ISGs) involved in TLR7 and type I IFN receptor signaling, including *Irf7*, *Viperin* and *Stat1* (Fig 2E). Intriguingly, CRE exposure alone significantly down-regulated the expression of *Viperin*, a component of the TLR7 signaling cascade in pDCs[34]. Although TLR7-mediated activation of pDC is critical for host defense against acute PVM infection[20], CRE exposure did not affect pDC numbers in the lung (Fig E3B in online repository).

Type-2 inflammation and ASM remodeling is elevated in PVM/CRE co-exposed mice in early-life

Allergen exposure is well known to induce the release of IL-33 to promote type-2 inflammation[35]. Analyzing IL-33 protein expression across the time course of infection revealed a significant increase in the lung homogenates at 3 dpi (sampling two hours after CRE exposure) and at 7 dpi in the co-exposed mice, but not those exposed to PVM alone (Fig 3A, upper panel). Although CRE exposure did not increase lung IL-33 expression at 3 dpi, it did increase airway luminal IL-33 measured in the BALF at this time, both in PVM infected mice and non-infected mice (Fig 3B). Consistent with other reports[36], under homeostatic conditions IL-33 was expressed predominantly in resident myeloid cell populations and alveolar (but not airway) epithelial cells (Fig 3C, top left panel). However, by 7 dpi IL-33-immunoreactive AECs were evident in PVM alone and PVM/CRE exposed mice (Fig 3C and Fig E3C), which was notable as a second phase of IL-33 release occurred at 10 dpi (Fig 3B). In contrast to IL-33, the expression of IL-25 and TSLP was unaffected by PVM and/or CRE exposure (data not shown). Critically, the IL-33 response was associated with increased numbers of type-2 ILCs and eosinophils (CD4+ and CD8+ T cell numbers were unaffected; data not shown) and type-2 cytokine expression (Fig 3D-F and Fig E4A online repository). Using IL-4/IL-13 reporter mice[27], we revealed that CD8+, but not CD4+, T cells contributed to IL-4 and IL-13 production. However, the majority of type-2 ILCs were IL-13-positive, and the proportion of IL-13-expressing type-2 ILCs, but not CD4+ or CD8+ T cells, increased in PVM/CRE co-exposed mice (Fig E4B online repository). Similar to our observations of ASM remodeling in later-life (Fig

1G), PVM infection or CRE exposure alone had no effect on ASM growth, while co-exposure induced a 3-fold increase in ASM area (Fig 3G).

Elevated viral load is not sufficient to induce type 2 inflammation and ASM remodeling.

To address whether elevated viral load was causally related to the development of ASM growth, we first inoculated mice with a 10x higher dose of PVM. While this increased the viral load and induced severe illness and mortality (Fig 4A-B), it was not sufficient to increase IL-33 release at 3 dpi (even when the dose was increased 100-fold (data not shown)) or induce ASM growth (Fig 4C-D). We then assessed whether house dust mite (HDM), was able to affect viral load and ASM growth at 7 and 10 dpi respectively (when these pathologies peaked). Substitution of CRE with HDM significantly increased viral load similar to CRE co-exposure but had no effect on ASM growth (Fig 4E-F), consistent with a lack of effect on anti-viral cytokine expression, type-2 ILCs in the lungs or the release of IL-33 (Fig 4G-I). Notably, HDM induced IL-33 release was detectable at 7 dpi, consistent with the findings of others (data not shown)[28, 31, 37-39]. Since the level of endotoxin in the CRE was high (395 EU per 100 μg protein), we co-exposed mice to PVM and an equivalent dose of LPS. LPS induced a massive IFN-α response and lowered viral load (Fig 4H-I), suggesting LPS contamination of CRE was not the cause of impaired antiviral immunity. Taken together, our findings suggested that ASM growth and the onset of type 2 inflammation was associated with an IFN-α/λ^{low}IL-33^{high} cytokine micro-environment rather than viral load.

Anti-IL-33 prevents type-2 inflammation and remodeling in response to virus and allergen co-exposure in early and later-life.

To assess the contribution of IL-33, mice were treated with a neutralizing antibody in both early and later-life (Fig E5A in online repository). Whereas mice treated with an isotype-matched control developed all of the hallmark features of asthma, treatment with anti-IL-33 abolished these features (Fig E5B-E in online repository). Similarly, anti-IL-33 treatment in early life ablated ASM growth

and the onset of type-2 inflammation (Fig 5A-D, Fig E5F in online repository). As expected, anti-IL-33 had no effect in mice infected with PVM alone.

IL-33 is a negative regulator of innate antiviral immunity.

We hypothesized that CRE might dampen innate antiviral immunity via the release of IL-33. Strikingly, anti-IL-33 reversed the elevated viral burden, dampened IFN-α and IFN-λ production and attenuated ISG expression caused by CRE exposure, but did not alter pDC or CD8 T cell numbers in the lung (Fig 6A-C, Fig E5G-H in online repository). In contrast, anti-IL-33 had no effect on the antiviral response in mice infected with PVM alone. CRE-induced IL-33 release occurs downstream of ATP-mediated purinergic receptor activation[35]. In our model, treatment with apyrase (to catalyse the hydrolysis of ATP) significantly decreased IL-33 in BALF (2 hours after CRE exposure, Fig E6A in online repository), and significantly lowered viral load at 7 dpi in the airway epithelium of PVM/CRE co-exposed mice (Fig 6D). Treatment with the broad-spectrum P2R antagonist PPADS had the same effect (Fig E6A-B), further implicating nucleoside/purinergic receptor signaling in mediating IL-33 release. As with anti-IL-33, blocking IL-33 release recapitulated IFN-α production and ISG expression in the lung (Fig 6E-F), decreased IL-13 expression (data not shown) and ablated ASM growth (Fig 6G), again highlighting the protective nature of an IFN-α/λ^{high}IL-33^{low} cytokine environment. This led us to question whether IFN-α suppresses IL-33-induced cytokine production by type-2 ILCs. Notably, FACS-purified type 2 ILCs expressed the type I IFN receptor (IFNAR; Fig E4A in online repository) and produced less IL-5 and IL-13 in response to IL-2/IL-33 stimulation when pretreated with IFN-α (Fig 6H). This response was unrelated to cell death (Fig E6C-D in online repository), however we observed that IFN-α attenuated IL-2/IL-33-induced up-regulation of ST-2 (Fig 6I).

Exogenous IL-33 increases viral load and decreases IRAK1 expression and antiviral cytokine production by pDC

We next examined the effect of low-dose exogenous IL-33 during acute PVM infection. Similar to CRE, exposure to exogenous IL-33 (10 ng at 3, 4 and 5 dpi; i.n. route) during acute PVM infection did not affect the infiltration of pDC (Fig E7A-B in online repository), however it significantly diminished IFN-α and IFN-λ in the BALF, increased epithelial viral load, and ablated ISG expression in the lung (Fig 7A-D). Moreover, IL-33/PVM co-exposure significantly increased ASM growth, in contrast to IL-33 or PVM alone (Fig 7E). Lastly, we questioned whether IL-33 affects TLR7-mediated activation of pDC by rapidly depleting the intracellular adaptor molecules interleukin-1 receptor associated kinase 1 (IRAK1) and viperin[40, 41]. Consistent with this possibility, ST2 was expressed on pDCs in bone marrow, lung and mediastinal lymph nodes (Fig 7F). Notably, in PVM/CRE co-exposed mice, intracellular IRAK1 and viperin expression in pDC was significantly diminished within 2 hours of CRE administration (Fig 7G). To directly assess the role of IL-33, we stimulated pDCs *in vitro* with IL-33. As shown *in vivo*, IRAK1 expression by pDCs was rapidly decreased (Figure 7H). Additionally, IL-33 treatment significantly diminished the production of IFN-α (Figure 7I) and IL-12p40 (data not shown) production in response to TLR7 stimulation. Collectively, these data suggest that IL-33 negative regulates the early antiviral response by inducing a state of TLR7 hypo-responsiveness in pDC.

Discussion

IL-33 and its receptor, ST2, have been reproducibly identified in genetic studies as asthma susceptibility loci, and clinical and experimental studies have revealed a preeminent role for IL-33 in the development and expansion of Th2 immunity via the activation of CD4+ Th2 cells, type-2 ILCs and various type-2 effector cells. In the present study we extend this paradigm to show that IL-33 dampens antiviral cytokine production, thus removing an inhibitory tonic and establishing a cytokine microenvironment that is conducive for the expansion of type-2 inflammation and ASM growth. Critically, using a novel preclinical model of asthma, we demonstrate that this dual activity

of IL-33 underlies the synergistic effect of respiratory virus and allergen exposures on the development and progression of asthma.

We repeatedly inoculated mice with low-dose virus and allergen to better simulate the natural course of events, and demonstrated that each of these environmental exposures, in both early and later-life, was necessary to maximally induce all of the cardinal features of asthma. Several investigators have developed experimental mouse models of virus/allergen co-exposure to show that a respiratory virus infection facilitates sensitization to an otherwise innocuous allergen; however in these models, as in ours, allergic sensitization was not apparent until after allergen challenge. We note that analysis from one birth cohort study found that allergic sensitization precedes rhinovirus induced wheezing[42]. However, it is important to note that while rhinovirus-associated illness occurs in older children, severe RSV bronchiolitis often occurs in the first year of life, when aeroallergen-specific IgE titers remain low[10]. Since an antibody-mediated response did not account for the predisposing effect of CRE in early-life, we questioned whether the primary allergen exposure altered the course of the respiratory virus infection. Unexpectedly, we found that the CRE exposure attenuated antiviral cytokine production and doubled the viral load in the airway epithelium. Treatment of PVM/CRE co-exposed mice with anti-IL-33 or apyrase, restored IFN-α production and decreased the viral burden to levels observed with PVM alone, while substitution of CRE with exogenous IL-33 attenuated IFN-α production and increased viral load, implicating IL-33 as a potent suppressor of antiviral immunity. Mechanistically, we found that IRAK1 and viperin expression by pDC was lower *in vivo* in PVM/CRE co-exposed mice and IRAK1 lower *in vitro* following IL-33 treatment. Significantly, IL-33 impaired the production of IFN-α by pDC, consistent with our earlier report that TLR7 hypo-responsiveness is a feature of asthma[22]. Additionally, CRE or IL-33 exposure decreased *Viperin* and *Irf7* gene expression *in vivo*, while anti-IL-33 or apyrase treatment attenuated this down-regulation. Because viperin interacts with IRAK1 to induce the nuclear translocation of IRF7 and downstream IFN production by pDCs[34], our

findings illustrate that IL-33 negatively regulates TLR7 signaling by at least three key points: viperin, IRAK1 and IRF7.

Presently, the role of type I and III IFNs in asthma pathogenesis is highly contentious. The first reports of impaired IFN–β and IFN-λ production by *ex vivo* virus-stimulated AECs from asthmatics[13, 14] have not been universally replicated by other investigators[16-18], leading to suggestions that the phenotype is only present in a subpopulation of patients or may stem from the cytokine milieu[43]. In light of our findings, these concepts may not be mutually exclusive since the IL-33 receptor IL-1 receptor-like 1, a common susceptibility loci for asthma[25], is expressed on AECs[44], and RV infected AECs secrete IL-33[45]. Accordingly, it will be important to test whether the increased viral load in the nasal lavage, reported by Jackson *et al*[45] is related to the suppressive effects of IL-33 on antiviral immunity.

The phenotype of our early-life model shows a number of striking similarities to pediatric patients with severe therapy-resistant asthma, including impaired type I and III IFN production, increased collagen deposition, and eosinophilic inflammation[46-48]. It remains to be established whether the aetiology of disease in this patient group relates to severe/frequent vLRIs; however, it is noteworthy that they present with elevated IL-33 expression[47], and therefore have an IFN-α/λ^{low}IL-33^{high} cytokine microenvironment, as observed in our model. We and others have shown that type I and III IFNs suppress CD4+ Th2 cytokine production[49], and here we show that IFN-α suppressed IL-33 induced type-2 cytokine production by type 2 ILCs, in part by preventing the up-regulation of ST2. Our findings highlight an important counter-regulatory process whereby IL-33 suppresses antiviral cytokine production. Such systems are critically dependent on the timing of expression, emphasizing the need to tightly regulate the release of pre-stored IL-33. Evidently, if the release of IL-33 is triggered inadvertently, as we show here in response to CRE exposure, this can have profound short- and long-term effects which may be exacerbated in individuals with a gain of

function single nucleotide polymorphism in the IL-33 or IL1RL1 gene[50]. The importance of timing was further emphasized when we switched CRE with HDM; although HDM did induce IL-33 as others have shown, the response was too slow to affect the antiviral response. Thus, we predict that exposure to HDM at the time of inoculation would predispose to viral bronchiolitis and subsequent asthma.

In the naïve mouse lung, IL-33 is primarily expressed by alveolar epithelial cells, however in response to ovalbumin challenge several different types of hematopoietic cells also produce IL-33[36]. In our model, PVM/CRE co-exposure of neonatal mice induced IL-33 release in a biphasic manner, peaking at 3 dpi (i.e. 2 hr after CRE exposure) and then at 10 dpi. Notably, CRE alone induced IL-33 release at 3 dpi but not 10 dpi, PVM infection alone induced IL-33 release at 10 dpi only, while expression at both time points was significantly elevated in co-exposed mice. PVM infection increased IL-33 expression in AECs, though not until 7 dpi, implicating infiltrating inflammatory cells or alveolar epithelial cells as the source of IL-33 at 3 dpi. This release of IL-33 was ATP-dependent[35]; however, the late release, which was associated with PVM infection, may have involved a separate mechanism. Indeed, recent reports have shown that the release of active IL-33 can also occur downstream of necroptosis, a programmed form of necrotic cell death, that can be initiated by viral activation of TLR3[51], consistent with the apparent association between late IL-33 release and viral load in our model at 10 dpi.

A striking feature of our model was the development of ASM growth, which to our knowledge has not been observed previously in an experimental model of virus-induced asthma. Furthermore, we demonstrated that this hallmark pathology of asthma began to develop in early life, consistent with a recent clinical report where ASM changes were evident in preschool age children with wheeze who are later diagnosed with asthma[52]. In fact, evidence of ASM proliferation is infrequent in subjects with established asthma[53], emphasizing the need for new therapies to target prevention in

early-life, rather than resolution of ASM mass in later-life. Neutralization or blockade of IL-33 release significantly decreased the development of ASM remodeling, together with other features of asthma, in both early- and later-life. IL-33 has been shown to directly induce collagen synthesis from fibroblasts[47], however ASM cells do not express ST2[44], and hence it is likely that the effects of IL-33 on ASM growth in our model were indirect, perhaps being mediated via the activation of type-2 ILCs and/or eosinophils.

In summary, we have developed a novel model to study the molecular processes that underlie the synergistic relationship between vLRI and allergen exposure, and the onset of asthma. CRE exposure rapidly induces the release of IL-33, which down-regulates components of the TLR7 signaling pathway causing TLR7 hypo-responsiveness in pDC. The ensuing IFN-α/λ^{low}IL-33^{high} cytokine microenvironment allows for the expansion of type-2 inflammation and increased ASM growth in early-life. This in turn leads to persistent alterations to resident airway cells and/or immune cells necessary for disease progression following viral and allergen challenge in later-life. Thus, emerging therapies aimed at targeting IL-33 will not only decrease Th2 inflammation, but will likely boost innate antiviral immunity.

REFERENCES

1. James AL, Pare PD, Hogg JC. The mechanics of airway narrowing in asthma. Am Rev Respir Dis 1989; 139:242-6.
2. Lambert RK, Wiggs BR, Kuwano K, Hogg JC, Pare PD. Functional significance of increased airway smooth muscle in asthma and COPD. J Appl Physiol 1993; 74:2771-81.
3. Holgate ST, Davies DE, Lackie PM, Wilson SJ, Puddicombe SM, Lordan JL. Epithelial-mesenchymal interactions in the pathogenesis of asthma. J Allergy Clin Immunol 2000; 105:193-204.
4. Fichtner-Feigl S, Strober W, Kawakami K, Puri RK, Kitani A. IL-13 signaling through the IL-13alpha2 receptor is involved in induction of TGF-beta1 production and fibrosis. Nat Med 2006; 12:99-106.
5. Neill DR, Wong SH, Bellosi A, Flynn RJ, Daly M, Langford TK, et al. Nuocytes represent a new innate effector leukocyte that mediates type-2 immunity. Nature 2010; 464:1367-70.
6. McKenzie Andrew NJ, Spits H, Eberl G. Innate Lymphoid Cells in Inflammation and Immunity. Immunity 2014; 41:366-74.
7. Stein RT, Sherrill D, Morgan WJ, Holberg CJ, Halonen M, Taussig LM, et al. Respiratory syncytial virus in early life and risk of wheeze and allergy by age 13 years. Lancet 1999; 354:541-5.
8. James KM, Gebretsadik T, Escobar GJ, Wu P, Carroll KN, Li SX, et al. Risk of childhood asthma following infant bronchiolitis during the respiratory syncytial virus season. J Allergy Clin Immunol 2013; 132:227-9.
9. Sigurs N, Bjarnason R, Sigurbergsson F, Kjellman B. Respiratory syncytial virus bronchiolitis in infancy is an important risk factor for asthma and allergy at age 7. Am J Respir Crit Care Med 2000; 161:1501-7.
10. Holt PG, Rowe J, Kusel M, Parsons F, Hollams EM, Bosco A, et al. Toward improved prediction of risk for atopy and asthma among preschoolers: a prospective cohort study. J Allergy Clin Immunol 2010; 125:653-9.
11. Holt PG, Sly PD. Viral infections and atopy in asthma pathogenesis: new rationales for asthma prevention and treatment. Nat Med 2012; 18:726-35.
12. Oddy WH, de Klerk NH, Sly PD, Holt PG. The effects of respiratory infections, atopy, and breastfeeding on childhood asthma. Eur Respir J 2002; 19:899-905.
13. Contoli M, Message SD, Laza-Stanca V, Edwards MR, Wark PA, Bartlett NW, et al. Role of deficient type III interferon-lambda production in asthma exacerbations. Nat Med 2006; 12:1023-6.

14. Wark PA, Johnston SL, Bucchieri F, Powell R, Puddicombe S, Laza-Stanca V, et al. Asthmatic bronchial epithelial cells have a deficient innate immune response to infection with rhinovirus. J Exp Med 2005; 201:937-47.
15. Gill MA, Bajwa G, George TA, Dong CC, Dougherty, II, Jiang N, et al. Counterregulation between the FcepsilonRI pathway and antiviral responses in human plasmacytoid dendritic cells. J Immunol 2010; 184:5999-6006.
16. Spann KM, Baturcam E, Schagen J, Jones C, Straub CP, Preston FM, et al. Viral and host factors determine innate immune responses in airway epithelial cells from children with wheeze and atopy. Thorax 2014.
17. Sykes A, Macintyre J, Edwards MR, Del Rosario A, Haas J, Gielen V, et al. Rhinovirus-induced interferon production is not deficient in well controlled asthma. Thorax 2014; 69:240-6.
18. Bochkov YA, Hanson KM, Keles S, Brockman-Schneider RA, Jarjour NN, Gern JE. Rhinovirus-induced modulation of gene expression in bronchial epithelial cells from subjects with asthma. Mucosal Immunol 2010; 3:69-80.
19. Swiecki M, Gilfillan S, Vermi W, Wang Y, Colonna M. Plasmacytoid dendritic cell ablation impacts early interferon responses and antiviral NK and CD8(+) T cell accrual. Immunity 2010; 33:955-66.
20. Davidson S, Kaiko G, Loh Z, Lalwani A, Zhang V, Spann K, et al. Plasmacytoid dendritic cells promote host defense against acute pneumovirus infection via the TLR7-MyD88-dependent signaling pathway. J Immunol 2011; 186:5938-48.
21. Lynch JP, Mazzone SB, Rogers MJ, Arikkatt JJ, Loh Z, Pritchard AL, et al. The plasmacytoid dendritic cell: a cell at the cross-roads in asthma. Eur Respir J 2013.
22. Roponen M, Yerkovich ST, Hollams E, Sly PD, Holt PG, Upham JW. Toll-like receptor 7 function is reduced in adolescents with asthma. Eur Respir J 2010; 35:64-71.
23. Bem RA, Domachowske JB, Rosenberg HF. Animal models of human respiratory syncytial virus disease. Am J Physiol Lung Cell Mol Physiol 2011; 301:L148-56.
24. Kaiko GE, Loh Z, Spann K, Lynch JP, Lalwani A, Davidson S, et al. TLR7 gene deficiency and early-life Pneumovirus infection interact to predispose toward the development of asthma-like pathology in mice. J Allergy Clin Immunol 2013; 131:1331-39.
25. Traister RS, Uvalle CE, Hawkins GA, Meyers DA, Bleecker ER, Wenzel SE. Phenotypic and genotypic association of epithelial IL1RL1 to human TH2-like asthma. J Allergy Clin Immunol 2015; EPub ahead of print.
26. Savenije OE, Mahachie John JM, Granell R, Kerkhof M, Dijk FN, de Jongste JC, et al. Association of IL33–IL-1 receptor–like 1 (IL1RL1) pathway polymorphisms with wheezing

phenotypes and asthma in childhood. Journal of Allergy and Clinical Immunology 2014; 134:170-7.

27. Huang Y, Guo L, Qiu J, Chen X, Hu-Li J, Siebenlist U, et al. IL-25-responsive, lineage-negative KLRG1(hi) cells are multipotential 'inflammatory' type 2 innate lymphoid cells. Nat Immunol 2015; 16:161-9.

28. Ullah MA, Loh Z, Gan WJ, Zhang V, Yang H, Li JH, et al. Receptor for advanced glycation end products and its ligand high-mobility group box-1 mediate allergic airway sensitization and airway inflammation. J Allergy Clin Immunol 2014; 134:440-50.

29. Phipps S, Hansbro N, Lam CE, Foo SY, Matthaei KI, Foster PS. Allergic sensitization is enhanced in early life through toll-like receptor 7 activation. Clin Exp Allergy 2009; 39:1920-8.

30. Hammad H, Chieppa M, Perros F, Willart MA, Germain RN, Lambrecht BN. House dust mite allergen induces asthma via Toll-like receptor 4 triggering of airway structural cells. Nat Med 2009; 15:410-6.

31. Willart MA, Deswarte K, Pouliot P, Braun H, Beyaert R, Lambrecht BN, et al. Interleukin-1alpha controls allergic sensitization to inhaled house dust mite via the epithelial release of GM-CSF and IL-33. J Exp Med 2012; 209:1505-17.

32. Guo L, Huang Y, Chen X, Hu-Li J, Urban Jr JF, Paul WE. Innate immunological function of TH2 cells in vivo. Nat Immunol 2015; advance online publication.

33. Aherne W, Bird T, Court SD, Gardner PS, McQuillin J. Pathological changes in virus infections of the lower respiratory tract in children. J Clin Pathol 1970; 23:7-18.

34. Saitoh T, Satoh T, Yamamoto N, Uematsu S, Takeuchi O, Kawai T, et al. Antiviral protein Viperin promotes Toll-like receptor 7- and Toll-like receptor 9-mediated type I interferon production in plasmacytoid dendritic cells. Immunity 2011; 34:352-63.

35. Kouzaki H, Iijima K, Kobayashi T, O'Grady SM, Kita H. The danger signal, extracellular ATP, is a sensor for an airborne allergen and triggers IL-33 release and innate Th2-type responses. J Immunol 2011; 186:4375-87.

36. Hardman CS, Panova V, McKenzie ANJ. IL-33 citrine reporter mice reveal the temporal and spatial expression of IL-33 during allergic lung inflammation. European Journal of Immunology 2013; 43:488-98.

37. Tjota MY, Williams JW, Lu T, Clay BS, Byrd T, Hrusch CL, et al. IL-33-dependent induction of allergic lung inflammation by FcgammaRIII signaling. J Clin Invest 2013; 123:2287-97.

38. Chu DK, Llop-Guevara A, Walker TD, Flader K, Goncharova S, Boudreau JE, et al. IL-33, but not thymic stromal lymphopoietin or IL-25, is central to mite and peanut allergic sensitization. J Allergy Clin Immunol 2013; 131:187-200.e1-8.
39. Llop-Guevara A, Chu DK, Walker TD, Goncharova S, Fattouh R, Silver JS, et al. A GM-CSF/IL-33 pathway facilitates allergic airway responses to sub-threshold house dust mite exposure. PLoS One 2014; 9:e88714.
40. Liu YC, Simmons DP, Li XL, Abbott DW, Boom WH, Harding CV. TLR2 signaling depletes IRAK1 and inhibits induction of type I IFN by TLR7/9. J Immunol 2012; 188:1019-26.
41. Sandig H, Jobbings CE, Roldan NG, Whittingham-Dowd JK, Orinska Z, Takeuchi O, et al. IL-33 causes selective mast cell tolerance to bacterial cell wall products by inducing IRAK1 degradation. Eur J Immunol 2013; 43:979-88.
42. Jackson DJ, Evans MD, Gangnon RE, Tisler CJ, Pappas TE, Lee WM, et al. Evidence for a causal relationship between allergic sensitization and rhinovirus wheezing in early life. Am J Respir Crit Care Med 2012; 185:281-5.
43. Baraldo S, Saetta M, Barbato A, Contoli M, Papi A. Rhinovirus-induced interferon production in asthma. Thorax 2014; 69:772.
44. Yagami A, Orihara K, Morita H, Futamura K, Hashimoto N, Matsumoto K, et al. IL-33 mediates inflammatory responses in human lung tissue cells. J Immunol 2010; 185:5743-50.
45. Jackson DJ, Makrinioti H, Rana BMJ, Shamji BWH, Trujillo-Torralbo M-B, Footitt J, et al. IL-33-dependent Type 2 Inflammation During Rhinovirus-induced Asthma Exacerbations In Vivo. Am J Respir Crit Care Med 2014; EPub ahead of print.
46. Edwards MR, Regamey N, Vareille M, Kieninger E, Gupta A, Shoemark A, et al. Impaired innate interferon induction in severe therapy resistant atopic asthmatic children. Mucosal Immunol 2013; 6:797-806.
47. Saglani S, Lui S, Ullmann N, Campbell GA, Sherburn RT, Mathie SA, et al. IL-33 promotes airway remodeling in pediatric patients with severe steroid-resistant asthma. J Allergy Clin Immunol 2013; 132:676-85 e13.
48. Bossley CJ, Fleming L, Gupta A, Regamey N, Frith J, Oates T, et al. Pediatric severe asthma is characterized by eosinophilia and remodeling without T(H)2 cytokines. J Allergy Clin Immunol 2012; 129:974-82 e13.
49. Pritchard AL, Carroll ML, Burel JG, White OJ, Phipps S, Upham JW. Innate IFNs and plasmacytoid dendritic cells constrain Th2 cytokine responses to rhinovirus: a regulatory mechanism with relevance to asthma. J Immunol 2012; 188:5898-905.

50. Grotenboer NS, Ketelaar ME, Koppelman GH, Nawijn MC. Decoding asthma: translating genetic variation in IL33 and IL1RL1 into disease pathophysiology. J Allergy Clin Immunol 2013; 131:856-65.

51. Pasparakis M, Vandenabeele P. Necroptosis and its role in inflammation. Nature 2015; 517:311-20.

52. O'Reilly R, Ullmann N, Irving S, Bossley CJ, Sonnappa S, Zhu J, et al. Increased airway smooth muscle in preschool wheezers who have asthma at school age. J Allergy Clin Immunol 2012; 131:1024-32.

53. Stewart A. More muscle in asthma, but where did it come from? Am J Respir Crit Care Med 2012; 185:1035-7.

Figure legends

Figure. 1. Pneumovirus and allergen co-exposure synergise in both early- and later-life to promote type-2 inflammation and airway remodeling. (A) Study design. (B) Peribronchial eosinophils expressed per 100 μm of the epithelial basement membrane (BM). (C) Mucous-secreting cells as a % of airway epithelial cells (AECs). (D) Serum levels of cockroach-specific immunoglobulin (Ig) G1a measured by ELISA. (E) Top panel: peribronchial collagen area; bottom panel: representative micrograph (x400 magnification), scale bar = 50 μm, white arrow indicates collagen (blue). (F) Top panel: peribronchial periostin; bottom panel: representative micrograph (x1000 magnification), scale bar = 10μm, white arrow indicates periostin (pink). (G) Top panel: peribronchial airway smooth muscle (ASM) area; bottom panel: representative micrographs of ASM (x400 magnification), scale bar = 50 μm, white arrow indicates ASM (pink). Data are mean ± SEM, representative of three independent experiments, n=6-9 mice per group. * $p<0.05$, ** $p<0.01$, *** $p<0.001$ compared with vehicle mice. $^{\#}$ $p<0.05$, $^{\#\#}$ $p<0.01$, $^{\#\#\#}$ $p<0.001$ compared with PVM/CRE/PVM/CRE mice.

Figure. 2. Early-life CRE exposure increases viral load and dampens antiviral cytokine production. (A) Viral load in airway epithelial cells (AEC) detected by immunohistochemistry and enumerated as % of total AECs. (B) Oedema in the lung parenchyma. (C) Weight gain. (D) Interferon (IFN)-α, IFN-λ and IFN-γ in bronchoalveolar lavage fluid (BALF) and IL-12p40 in lung homogenate. (E) mRNA expression of IRF7, Viperin and STAT1 in lung, relative to vehicle treated mice. Data are mean ± SEM, representative of 2-3 experiments, n=4-6 mice per group. *compared with vehicle mice. $^{\#}$compared with PVM/CRE mice.

Figure. 3. Type-2 inflammation in early-life is elevated in PVM/CRE co-exposed mice. (A) IL-33 in lung homogenate and (B) bronchoalveolar lavage fluid (BALF). (C) Representative micrographs of IL-33 immunostaining plus DAPI (4',6-diamidino-2-phenylindole) counterstain, scale bar = 50 μm. (D) Type-2 innate lymphoid cells (ILCs) in lung (Lineage-, CD45+, CD90.2+, CD25+, ST2+). (E) Peribronchial eosinophils. (F) IL-5 and IL-13 in BALF. (G) ASM area. Data are mean ± SEM, representative of two independent experiments, n=6-8 mice per group. *compared with vehicle mice. $^{\#}$compared with PVM/CRE mice.

Figure 4. High viral load alone does not promote type 2 inflammation and airway remodeling. (A, E) Viral load in airway epithelial cells (AEC). (B) Survival curve of after i.n. infection with 1 plaque forming unit (pfu) or 10pfu of PVM. (C,G) IL-33 in bronchoalveolar lavage fluid (BALF). (D) ASM area. (H) Interferon (IFN)-α, IFN-λ, IFN-γ in BALF and IL-12p40 in lung homogenate. (I) Type-2 innate lymphoid cells (ILCs) in the lung. Data are mean ± SEM, representative of two independent experiments, n=6-8 mice per group. *compared with PVM mice. # compared with PVM/CRE mice.

Figure 5. Anti-IL-33 prevents type-2 inflammation and remodeling in response to PVM and CRE co-exposure in early--life. (A) Type-2 innate lymphoid cells in lung (ILCs). (B) IL-13 in bronchoalveolar lavage fluid (BALF). (C) Peribronchial eosinophils (D) ASM area. Data are mean ± SEM, representative of 2 experiments, n=6-7 mice per group. *compared with isotype-treated PVM/CRE co-exposed mice.

Figure. 6. IL-33 blockade in PVM/CRE co-exposed mice prevents excessive viral load and reverses dampened antiviral immunity induced by CRE. (A, D) Airway epithelial cell (AEC) viral load. (B, E) IFN-α and IFN-λ in bronchoalveolar lavage fluid (BALF); IL-12p40 in lung homogenate. (C, F) mRNA expression of interferon stimulated genes, relative to vehicle treated mice. (G) ASM area. (H) Type 2 ILCs were treated with IL-2 ± IFN-α for 30 min followed by

culture with IL-33 and IL-2 for 72 hours, before the supernatant was probed for IL-5 and IL-13; (I) ST-2 expression on cultured ILC2s; MFI, mean fluorescence intensity. Data are mean ± SEM, representative of two to three independent experiments, n=6-10 mice per group. *compared with PVM/CRE/isotype mice. * compared with PVM/CRE isotype mice or as indicated

Figure. 7. Exogenous IL-33 dampens IFN-α production and increases viral load by decreasing IRAK1 expression and antiviral cytokine production by pDC (A) IFN-α and (B) IFN-λ in bronchoalveolar lavage fluid (BALF). (C) Viral load in airway epithelial cells (AECs). (D) mRNA expression, relative to vehicle treated mice. (E) ASM area. (F) ST2 staining of bone marrow (BM), lung and mediastinal lymph node (LN) pDC (solid line). Fluorescence minus one for ST2 staining (grey). (G) IRAK1 and viperin intracellular expression in pDC *in vivo* at 2 hours post CRE administration. Mean fluorescence intensity (MFI). (H) Intracellular IRAK1 staining of bone marrow (BM)-pDC pre-incubated with vehicle (solid line) or IL-33 (3ng/ml, dotted line) for 0.5 h. Fluorescence minus one for IRAK staining (grey). (I) IFN-α production in BM-pDC cell culture supernatant Data are mean ± SEM, representative of two independent experiments, n=7 mice per group. N.D., not detected. * compared with PVM-alone mice or vehicle treated BM-pDC.

Acknowledgements

We thank Drs Nocka, Kasaian and Bloom (Pfizer, Inc) for the supply of anti-IL-33. We would also like to thank Dr Ashik Ullah (Queensland Institute of Medical Research) and Dr Ben Roediger (Centenary Institute) for technical assistance. This work was supported by an equipment grant (Rebecca L. Cooper Medical Research Foundation), an Australian Infectious Disease Research Excellence Award awarded to S.P., J.P.L and J.W.U., and an Australian Research Council Future Fellowship to S.P.

Author contributions

J.P.L., R.B.W., K.S., P.D.S., S.M., J.W.U., and S.P. designed research; J.P.L., R.B.W., J.S., Z.L., V.Z., performed research; K.S. and A.H., contributed reagents/analytic tools; J.P.L., R.B.W., J.S., analyzed data; and J.P.L., R.B.W., S.P., wrote the paper.

Figure 1

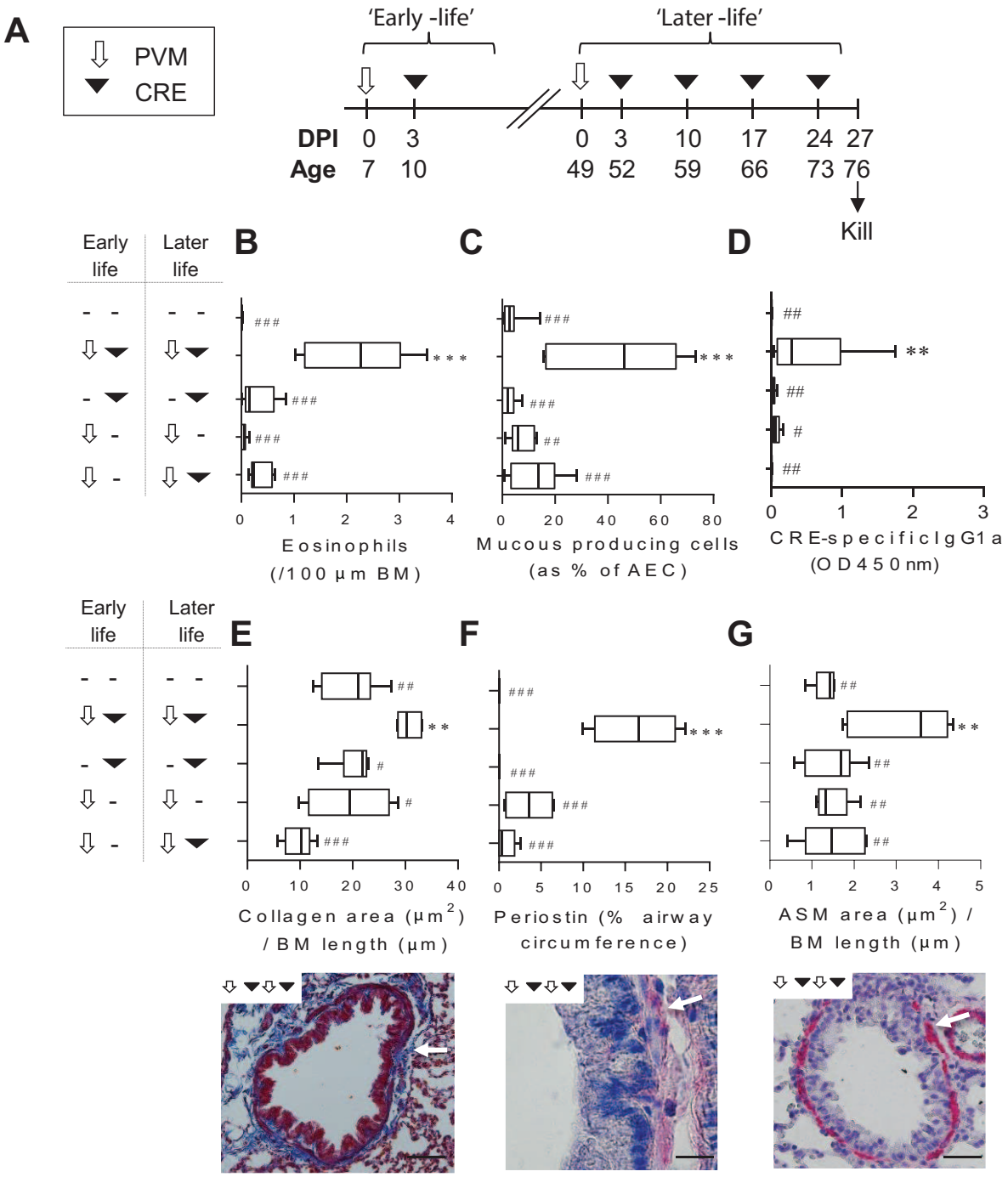
A
PVM
CRE
'Early -life'
'Later -life'
DPI 0 3 0 3 10 17 24 27
Age 7 10 49 52 59 66 73 76
Kill
Early life
Later life
B
C
D
Eosinophils (/100 µm BM)
Mucous producing cells (as % of AEC)
CRE-specific IgG1a (OD450nm)
E
F
G
Collagen area (µm²) / BM length (µm)
Periostin (% airway circumference)
ASM area (µm²) / BM length (µm)

Figure 2

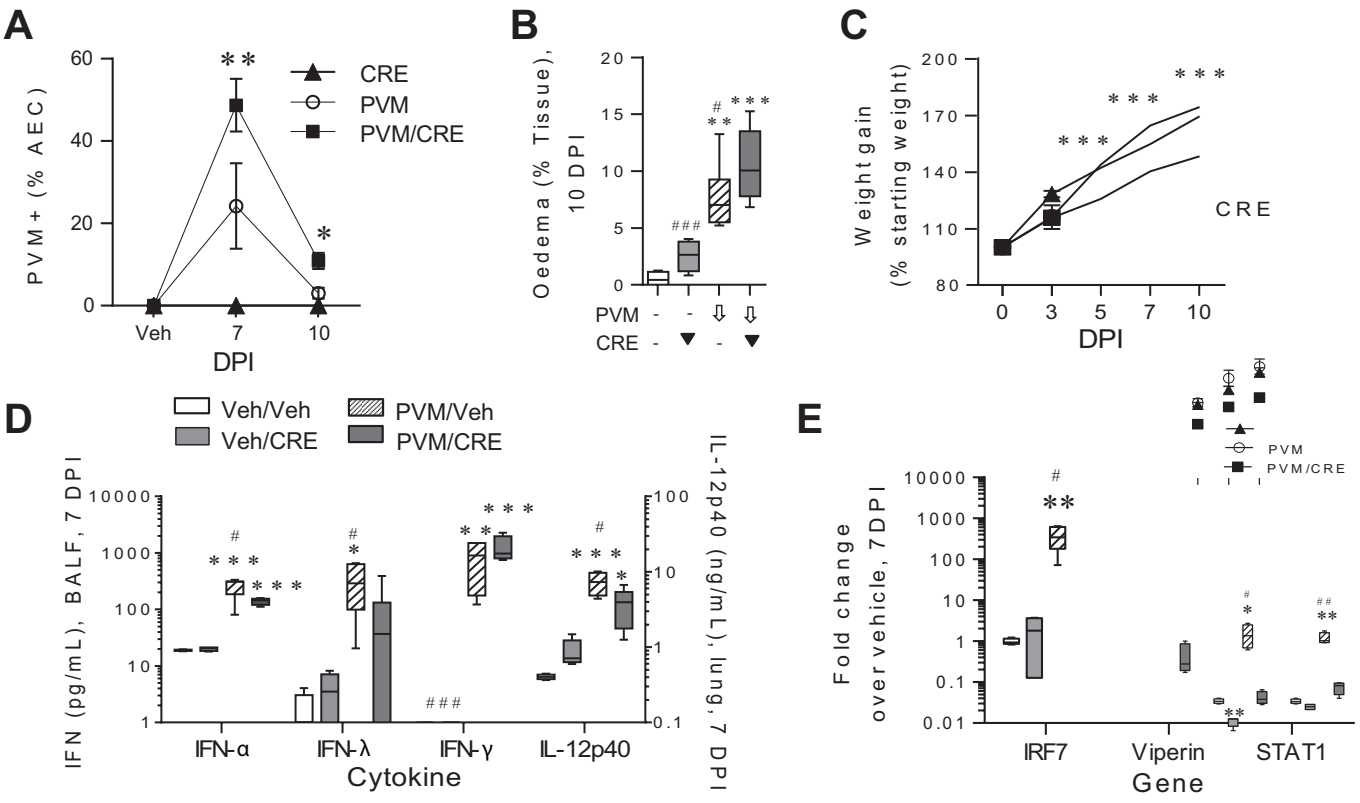
A
PVM+ (% AEC)
60
40
20
0
Veh
7
10
DPI
CRE
PVM
PVM/CRE
B
Oedema (% Tissue), 10 DPI
20
15
10
5
0
PVM
CRE
C
Weight gain (% starting weight)
200
170
140
110
80
0
3
5
7
10
DPI
CRE
D
Veh/Veh
Veh/CRE
PVM/Veh
PVM/CRE
IFN (pg/mL), BALF, 7 DPI
IL-12p40 (ng/mL), lung, 7 DPI
IFN-α
IFN-λ
IFN-γ
IL-12p40
Cytokine
E
Fold change over vehicle, 7DPI
PVM
PVM/CRE
IRF7
Viperin
STAT1
Gene

Figure 3

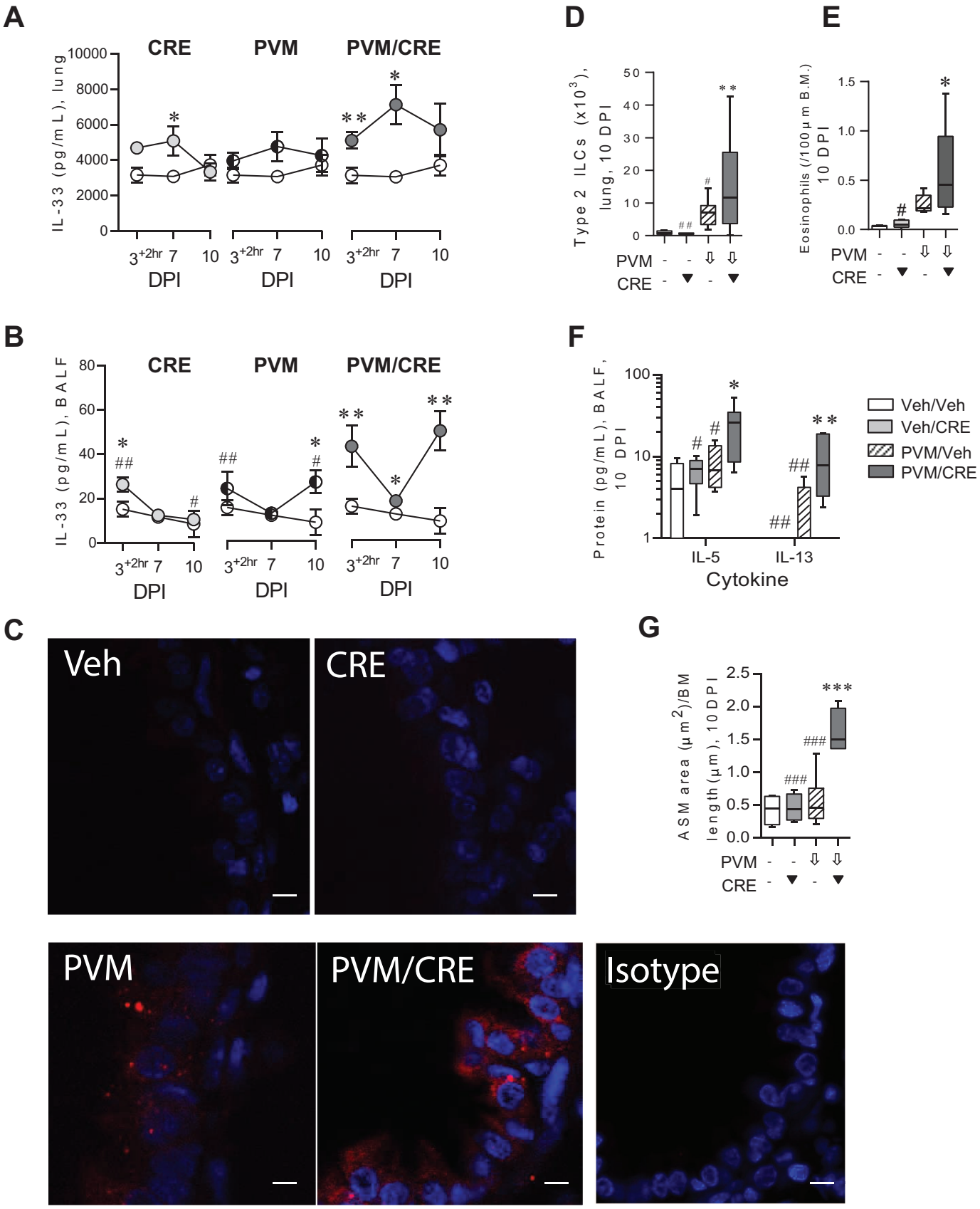
A
CRE
PVM
PVM/CRE
IL-33 (pg/mL), lung
DPI
B
IL-33 (pg/mL), BALF
C
Veh
CRE
PVM
PVM/CRE
Isotype
D
Type 2 ILCs (x10^3), lung, 10 DPI
PVM
CRE
E
Eosinophils (/100μm B.M.) 10 DPI
F
Protein (pg/mL), BALF, 10 DPI
IL-5
IL-13
Cytokine
Veh/Veh
Veh/CRE
PVM/Veh
PVM/CRE
G
ASM area (μm2)/BM length (μm), 10 DPI

Figure 4

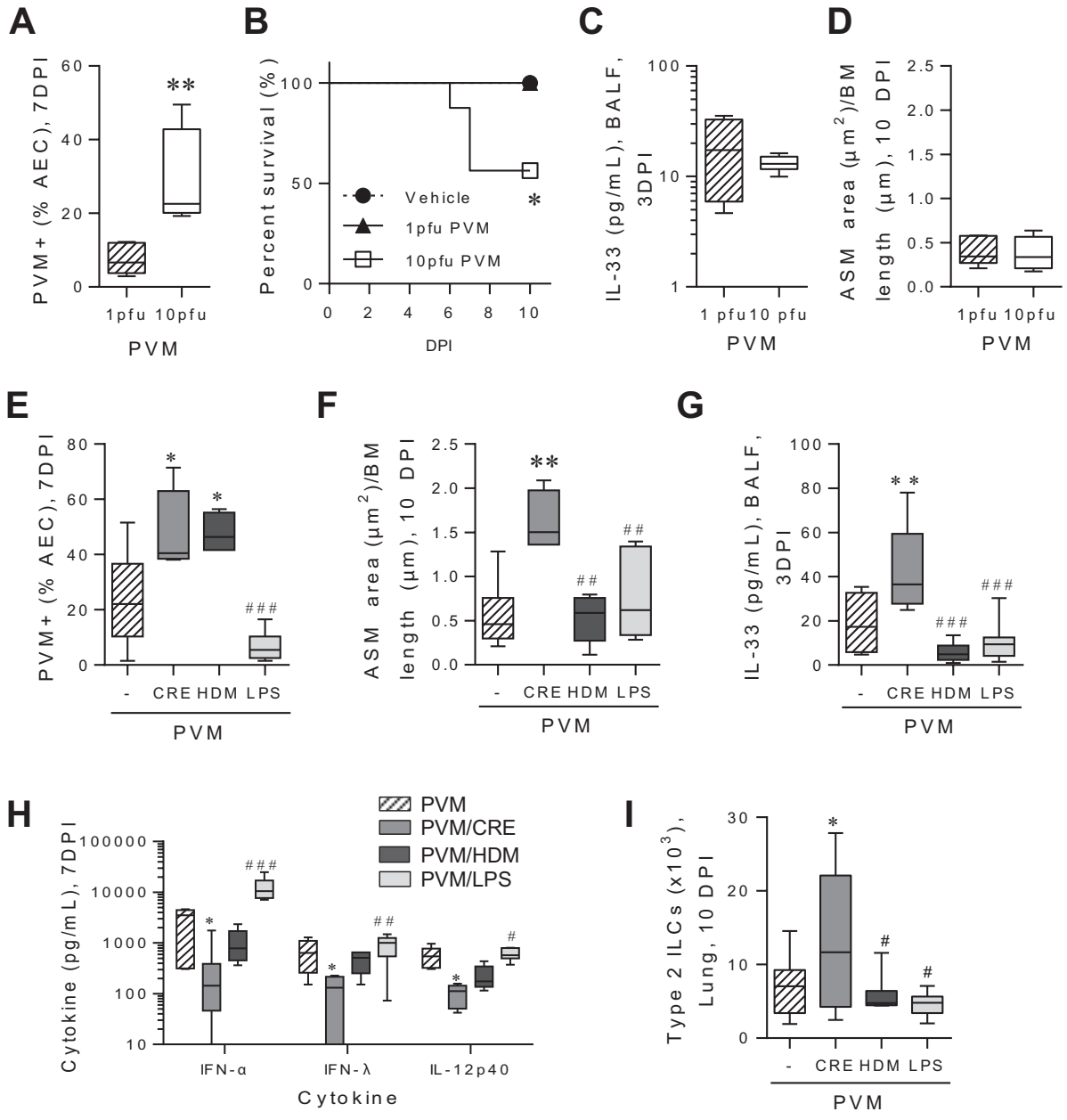
A
PVM+ (% AEC), 7DPI
1pfu 10pfu
PVM
B
Percent survival (%)
Vehicle
1pfu PVM
10pfu PVM
DPI
C
IL-33 (pg/mL), BALF, 3DPI
1 pfu 10 pfu
PVM
D
ASM area (μm²)/BM length (μm), 10 DPI
1pfu 10pfu
PVM
E
PVM+ (% AEC), 7DPI
- CRE HDM LPS
PVM
F
ASM area (μm²)/BM length (μm), 10 DPI
- CRE HDM LPS
PVM
G
IL-33 (pg/mL), BALF, 3DPI
- CRE HDM LPS
PVM
H
PVM
PVM/CRE
PVM/HDM
PVM/LPS
Cytokine (pg/mL), 7DPI
IFN-α
IFN-λ
IL-12p40
Cytokine
I
Type 2 ILCs (x10³), Lung, 10 DPI
- CRE HDM LPS
PVM

Figure 5

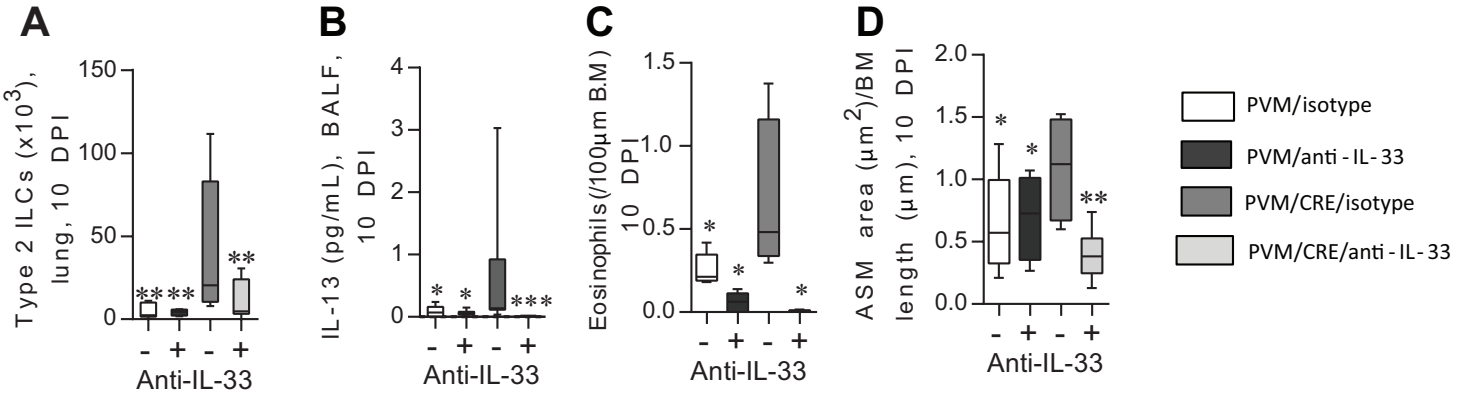
A
Type 2 ILCs (x10^3), lung, 10 DPI
150
100
50
0
**
**
**
- + - +
Anti-IL-33
B
IL-13 (pg/mL), BALF, 10 DPI
4
3
2
1
0
*
*
***
- + - +
Anti-IL-33
C
Eosinophils(/100µm B.M) 10 DPI
1.5
1.0
0.5
0.0
*
*
*
- + - +
Anti-IL-33
D
ASM area (µm^2)/BM length (µm), 10 DPI
2.0
1.5
1.0
0.5
0.0
*
*
**
- + - +
Anti-IL-33
PVM/isotype
PVM/anti - IL- 33
PVM/CRE/isotype
PVM/CRE/anti - IL- 33

Figure 6

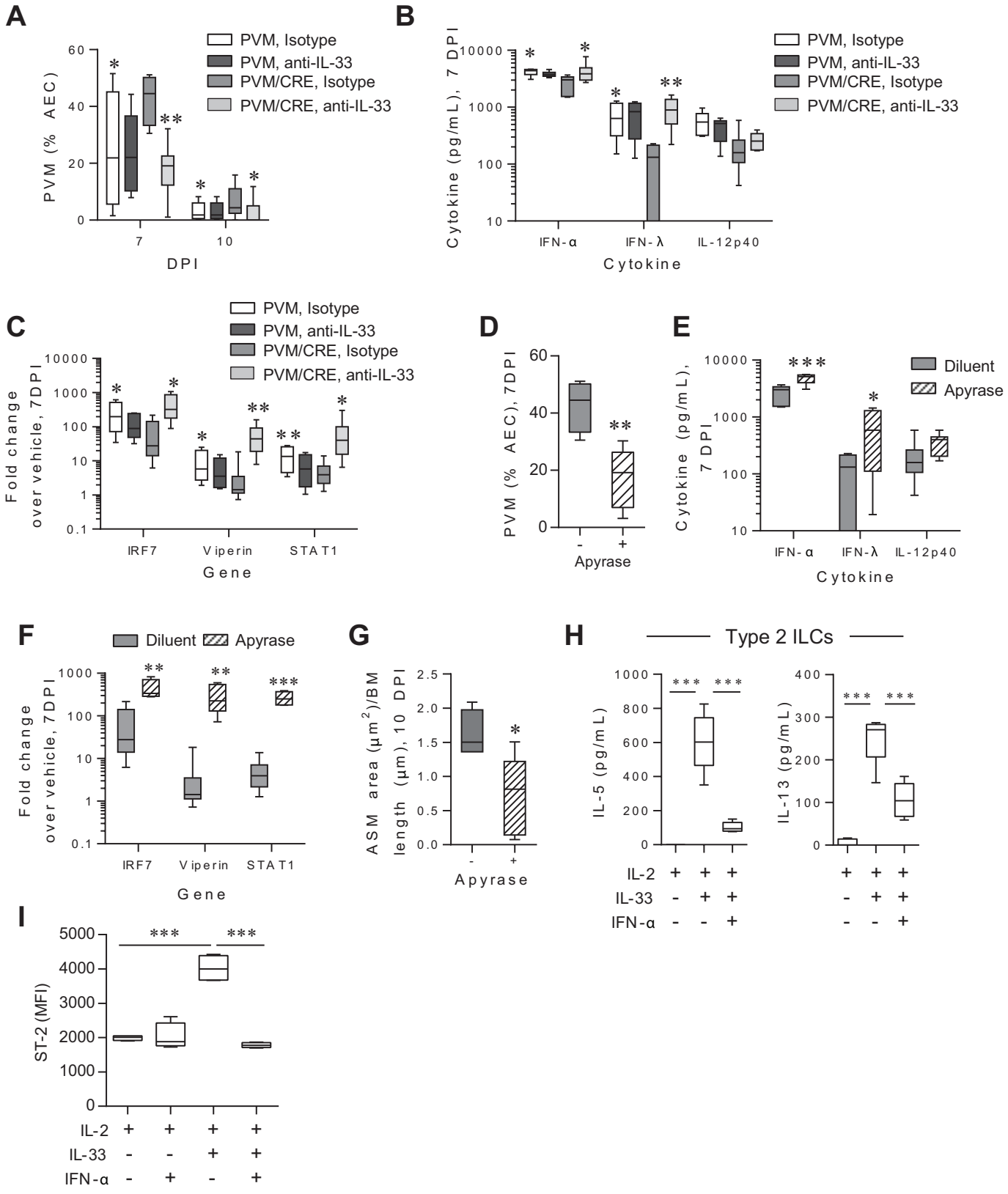
A
PVM, Isotype
PVM, anti-IL-33
PVM/CRE, Isotype
PVM/CRE, anti-IL-33
PVM (% AEC)
DPI
B
Cytokine (pg/mL), 7 DPI
IFN-α
IFN-λ
IL-12p40
Cytokine
C
Fold change over vehicle, 7DPI
IRF7
Viperin
STAT1
Gene
D
PVM (% AEC), 7DPI
Apyrase
E
Diluent
Apyrase
Cytokine (pg/mL), 7 DPI
F
G
ASM area (μm²)/BM length (μm), 10 DPI
H
Type 2 ILCs
IL-5 (pg/mL)
IL-13 (pg/mL)
IL-2
IL-33
IFN-α
I
ST-2 (MFI)

Figure 7

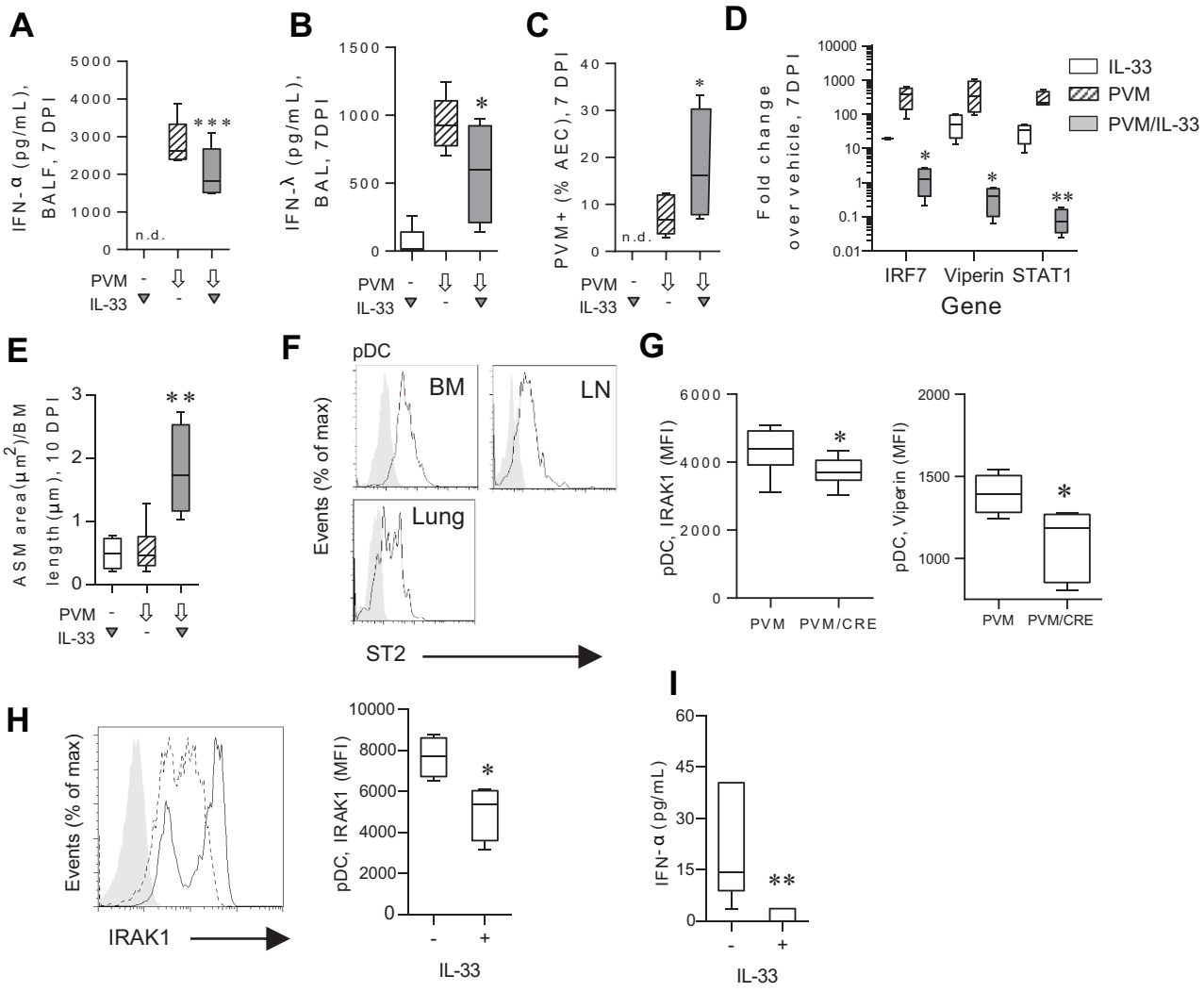
A
IFN-α (pg/mL), BALF, 7 DPI
5000
4000
3000
2000
1000
0
n.d.
***
PVM - ⇩ ⇩
IL-33 ▽ - ▽
B
IFN-λ (pg/mL), BAL, 7DPI
1500
1000
500
0
*
PVM - ⇩ ⇩
IL-33 ▽ - ▽
C
PVM+ (% AEC), 7 DPI
40
30
20
10
0
n.d.
*
PVM - ⇩ ⇩
IL-33 ▽ - ▽
D
Fold change over vehicle, 7DPI
10000
1000
100
10
1
0.1
0.01
*
*
**
IL-33
PVM
PVM/IL-33
IRF7
Viperin
STAT1
Gene
E
ASM area(μm²)/BM length(μm), 10 DPI
3
2
1
0
**
PVM - ⇩ ⇩
IL-33 ▽ - ▽
F
pDC
BM
LN
Lung
Events (% of max)
ST2
G
pDC, IRAK1 (MFI)
6000
4000
2000
0
*
PVM
PVM/CRE
pDC, Viperin (MFI)
2000
1500
1000
*
PVM
PVM/CRE
H
Events (% of max)
IRAK1
pDC, IRAK1 (MFI)
10000
8000
6000
4000
2000
0
*
-
+
IL-33
I
IFN-α (pg/mL)
60
45
30
15
0
**
-
+
IL-33

Online Repository

Aeroallergen-induced IL-33 predisposes to respiratory virus-induced asthma by dampening anti-viral immunity

Jason P. Lynch, PhD,[1*], Rhiannon B. Werder, BSc (Hons),[1*], Jennifer Simpson, B Biomed Sci (Hons),[1], Zhixuan Loh, B Biomed Sci (Hons),[1], Vivian Zhang, PhD,[1] Ashraful Haque, PhD,[2], Kirsten Spann, PhD,[2,3], Peter D. Sly, MD, PhD,[3,4], Stuart Mazzone, PhD,[1], John W. Upham, MD, PhD,[3,5,], and Simon Phipps, PhD,[1,3]

Online Methods

Induction of co-virus and allergen-induced asthma and associated perturbations.

Specific pathogen-free BALB/c mice or 4C13R mice [1] were inoculated with PVM (strain J3666; 1 pfu 'early life'; 20 pfu 'later life') or cockroach allergen extract (CRE, 1 µg, Greer Laboratories) as previously described [2, 3] and as outlined in the study design (Figure 1A). In some experiments, mice were exposed to HDM extract (5 µg or 100ug, Greer Laboratories) or LPS (186 pg, Sigma-Aldrich), recombinant IL-33 (10 ng, eBioscience), anti-IL-33/isotype control antibody (200 µg, Pfizer, Inc), apyrase (4 U/mL, Sigma-Aldrich) or pyridoxalphosphate-6-azophenyl-2',4'-disulfonic acid (PPADS, 100 µm, Sigma-Aldrich). All studies were approved by The University of Queensland Animal Ethics Committee.

Sample extraction and processing

Following euthanasia by pentobarbitone overdose, blood was obtained by cardiac puncture, centrifuged twice (13,000 rpm, 4°C) and the serum stored at -80^{o}C. A bronchoalveolar lavage

(BAL) was performed with 400 µL (neonate/'early life') or 600 µL (adult/'later life') of PBS. The BAL fluid was centrifuged at 5,000 rpm, 4°C for 5 min and the supernatant stored at -80°C until analysis by cytokine bead array (CBA) or ELISA. Lung lobes were excised and processed as previously described [4]. Briefly, the left lung lobe was processed immediately for flow cytometry and the superior right lobe fixed in 10% formalin neutral buffer overnight before storage in 70% ethanol. The post-caval and inferior lobes were pooled and snap frozen before mechanical digestion and clarification, followed by analysis by ELISA. The inferior right lobe was snap frozen before RNA extraction. All snap frozen lungs were stored at -80 °C.

Flow cytometry

Flow cytometry was performed on lung tissue digest cells as previously described [4]. Briefly, single cell suspensions were incubated with anti-FcγRIII/II (Fc block) for 15 min at 4°C then incubated with the following fluorochrome-conjugated antibodies at 4°C for 30 minutes: anti-mouse CD2-FITC (RM2-5), CD4–AF488 (RM4-5), Gr-1–AF488 (RB6-8C5), CD11c–AF488 (HL3), CD11b–AF488 (M1/70), B220-AF488 (RA36B2), CD3–AF488 (145-2C11) CD45RA-PE (14.8), B220-V500 (RA36B2), CD8a-PerCP (53-6.7), Sca1-PE (E13-161.7) (all BD Bioscience), CD19-AF488 (6D5), CD45-BV421 (30-F11), CD11b-BV421 (M1/70), ST-2-APC (DIH9), IFNAR (MAR1-5A3), ICOS-PE (7E.17G9), IL-7Ra-PE (SB/199) (all Biolegend), IL-17RB-PE-Cy7 (eBio17B7) (eBioscience) and Siglec-H-APC (511.3D3) (Miltenyi Biotec). 7-AAD (eBioscience) was used to exclude dead cells. For intracellular staining, cells were fixed and permeabilised using the BD Cytofix/Cytoperm kit as per the manufacturer's instructions, followed by staining with rabbit anti-mouse IRAK1 (D51G7, Cell Signalling) or anti-mouse Viperin (HM1016, Hycult) for 30 minutes. Cells were then washed followed by incubation with

goat anti-rabbit AF647 (Invitrogen) for 30 minutes. Samples were collected with an LSR Fortessa X-20 (BD Biosciences) and the data analysed with FACSDiva v8 (BD Biosciences) and FlowJo v8.8 (Treestar). Type 2 ILCs were identified as Lineage$^-$ (CD2, Gr-1, CD3, CD11b, B220, CD4, CD19), CD45$^+$, CD25$^+$, CD90.2$^+$, ST-2$^+$, ICOS$^+$, IL-7Ra$^+$, IL-17RB$^+$ (Fig E4A). pDCs were identified as CD11b$^-$, CD11c$^+$, CD45RA$^+$, B220$^+$, Siglec-H$^+$.

Histology and Immunohistochemistry

Paraffin-embedded lung sections were prepared as previously described [3]. Lung tissue sections were stained with Chromotrope 2R, Periodic acid-Schiff or Masson's Trichrome, to enumerate eosinophils, mucus-secreting cells and collagen deposition respectively. For immunohistochemistry, lung sections were pretreated with 10% normal goat serum for 30 min. Sections were probed with anti-IL-33 (AF3626, R&D), anti-PVM G protein (kindly provided by Dr Ulla Buchholz), anti-α-SM actin and anti-periostin (both Sigma-Aldrich) overnight at 4°C. Following incubation with appropriate secondary antibodies, immunoreactivity was developed with Fast Red (Sigma-Aldrich) and counterstained with Mayer's hematoxylin (bright field) or with 4',6-diamidino-2-phenylindole (DAPI, Sigma-Aldrich) (fluorescence). The percentage of PVM positive or mucous AECs was quantified in 5 airways per mouse (Scanscope XT, Aperio). Oedema was assessed by point counting of fluid-filled airspaces. Eosinophils were enumerated around the airways and expressed as cells per 100 mm of epithelial basement membrane. Airway smooth muscle mass and collagen deposition around the small airways (defined as a circumference <500 μm for neonates and <800 μm for mice aged >7 week) was measured using Scanscope XT software and expressed as area per μm of basement membrane. Periostin expression was quantified as a % of the airway circumference. Photomicrographs were taken at

400x and 1000x magnification using an Olympus BX-51 microscope with an Olympus DP-72 camera at room temperature and acquired using Olympus Image Analysis Software. IL-33 images were false colored using Adobe Photoshop CS6 software. Immunofluorescent images were taken using Diskovery Spinning disk confocal using Nikon Viewer software. Images were processed using Image J and Imaris software.

Measurement of protein expression

IL-33 and IFN-λ2/3 (R&D Systems), IL-12p40 and IFN-γ (Biolegend) and IL-5 (BD Biosciences) expression was quantified by ELISA. IFN-α (eBioscience) and IL-13 (Quantikine kit, R&D or Enhanced Sensitivity Flex Set, BD Biosciences) expression was quantified by CBA. IgG1a was detected in the serum using an in-house ELISA system [2].

Quantitative real time PCR

Total RNA was isolated from the inferior right lung lobe with TriReagent solution (Ambion) followed by phenol-chloroform extraction. DNAse digestion was performed with Turbo DNAse (Ambion), according to the manufacturer's instructions. Reverse transcription was performed using M-MLV reverse transcriptase and random primers (Invitrogen). qRT-PCR was performed with SYBR Green (Life Technologies) with the primers described in Table S1. Expression values were normalized to *Hprt* and expressed as fold change over vehicle mice, as described [3, 4].

Airway function assessment

AHR was measured as described previously [5]. Briefly, airways resistance was determined by forced oscillation technique (Flexivent, Scireq) in response to nebulized methacholine (0.3 to 10 mg/mL; Sigma-Aldrich).

Type-2 innate lymphoid cell culture and activation

Lungs were excised from PVM/CRE co-exposed mice at 10 dpi and digested by gentleMACS dissociation (Miltenyi Biotech). Type 2 ILCs (7-AAD$^-$ Lineage$^-$ CD45$^+$, CD25$^+$, CD90.2$^+$) were FACS-sorted to 96% purity (Fig E6C) using a BD FACS-Aria, and cultured in the presence of IL-2 (30 ng/mL, eBioscience). Cells (10,000/well) were pre-incubated with IFN-α (5000U/mL, Hycult Biotech) for 30 minutes, before stimulation with IL-33 (30 ng/mL, eBioscience) for 72 hours. Supernatant was collected and probed for cytokine production.

Plasmacytoid dendritic cell culture

Bone marrow-derived pDC were generated as described previously [3]. On day 8 of culture, pDC were pre-incubated with IL-33 (3 ng/mL, eBioscience) then stimulated with imiquimod (3 μg/mL, Sigma-Aldrich).

Statistical analyses

GraphPad Prism version 5.0 software (La Jolla, California) was used for all statistical analyses. A Student's t-test, one-way ANOVA with a Tukey post-hoc test or two-way ANOVA with a Sidak post-hoc test were applied as appropriate. A P value <0.05 was considered statistically significant.

Supplemental Figure Legends

Figure E1. Determination of CRE allergen dose (A) Study design. (B) Peribronchial eosinophils. BM, basement membrane. (C) Mucous-secreting cells. AEC, airway epithelial cells. Data are mean±SEM, representative of 2 experiments, n=5-9 mice per group.

Figure E2. Both virus and allergen challenge in later life are necessary for asthma progression. (A) Peribronchial eosinophils. Basement membrane (BM). (B) Mucous-secreting airway epithelial cells (AECs). (C) Cockroach-specific IgG1a in serum. (D) Collagen area. (E) ASM area. (F) Airway resistance (Rn) in response to increasing doses of methacholine (MCh), response at 10mg/mL shown. (G) Representative micrograph (x400 magnification) of peribronchial eosinophils (chromotrope 2R), scale bar = 50 μm, white arrows indicate eosinophils. Data are mean ± SEM, representative of three independent experiments, n=6-9 mice per group. * compared with vehicle mice. # compared with PVM/CRE/PVM/CRE mice. Dashed line denotes vehicle treated mice. Related to Figure 1.

Figure E3. Expression of virus and IL-33 in airway epithelial cells. (A) Representative micrographs of PVM immunostaining, scale bar = 50 μm, arrows indicate PVM+ airway epithelial cells. (B) pDC 7 days post infection, enumerated as CD11b- CD11c+ Siglec-H+ B220+ CD45RA+. (C) Quantification of airway epithelial cells (AECs) expressing IL-33 as % of AECs. (D) Bronchoalveolar lavage total and differential counts.

Figure E4. **Type 2 innate lymphoid cell and T cell responses**. (A) Representative scatter plots showing gating strategy for enumeration of type 2 ILCs and their immunophenotype in the lung. Grey filled histogram = fluorescence of minus one control for staining; solid line = expression of ILC2 markers in lung. Values are % of total lung cells. (B) ILC2, CD4- and CD8-T cell expression of IL-13 and IL-4 at 10 DPI in 4C13R mice. Values are % parent population.

Figure E5. Anti-IL-33 prevents type 2 inflammation and remodeling in response to virus and allergen co-exposure in later-life. (A) Study plan. (B) Airway resistance (Rn) in response to increasing doses of methacholine (MCh). (C) Mucous-secreting airway epithelial cells (AECs). (D) Peribronchial eosinophils. Basement membrane (BM). (E) ASM area. Data are mean ± SEM, representative of 2 experiments, n=6-7 mice per group. Dashed line denotes vehicle treated mice, solid line denotes PVM treated mice. (F) Bronchoalveolar lavage total and differential counts. (G) pDC number and (H) Sca-1+ CD8 T cells in the lung.

Figure E6. **Blockade of IL-33 release and type-2 ILC sort purity and viability in culture following stimulation.** (A) IL-33 in bronchoalveolar lavage (BALF), following treatment with apyrase or pyridoxalphosphate-6-azophenyl-2',4'-disulfonic acid (PPADS). (B) Viral load in airway epithelial cells and IL-12p40 in lung. (C) Representative scatter plots showing gating strategy for FACS sorting of lung type-2 ILCs. Values are % of parent population. (D) Viable (7-AAD-) type-2 ILCs following 3 day culture.

Figure E7. Exogenous IL-33 dampens IFN-α production and increases viral load (A) Study design. Mice were inoculated with PVM at 7 dpi, then exposed (i.n.) to 10 ng IL-33 3, 4 and 5 days later. (B) Plasmacytoid dendritic cell (pDC), (C) Type-2 ILC and (D) Eosinophil number in

the lung. (E-I) Bronchoalveolar lavage total and differential counts. (E) Representative scatter plots showing gating strategy for cultured pDCs.

Supplemental Table Legends

Table E1. Oligonucleotide sequences used in this study are shown.

Supplemental References

1. Huang Y, Guo L, Qiu J, Chen X, Hu-Li J, Siebenlist U, et al. IL-25-responsive, lineage-negative KLRG1(hi) cells are multipotential 'inflammatory' type 2 innate lymphoid cells. Nat Immunol 2015; 16:161-9.
2. Ullah MA, Loh Z, Gan WJ, Zhang V, Yang H, Li JH, et al. Receptor for advanced glycation end products and its ligand high-mobility group box-1 mediate allergic airway sensitization and airway inflammation. J Allergy Clin Immunol 2014; 134:440-50.
3. Davidson S, Kaiko G, Loh Z, Lalwani A, Zhang V, Spann K, et al. Plasmacytoid dendritic cells promote host defense against acute pneumovirus infection via the TLR7-MyD88-dependent signaling pathway. J Immunol 2011; 186:5938-48.
4. Kaiko GE, Loh Z, Spann K, Lynch JP, Lalwani A, Davidson S, et al. TLR7 gene deficiency and early-life Pneumovirus infection interact to predispose toward the development of asthma-like pathology in mice. J Allergy Clin Immunol 2013; 131:1331-39.
5. Phipps S, Lam CE, Kaiko GE, Foo SY, Collison A, Mattes J, et al. Toll/IL-1 signaling is critical for house dust mite-specific helper T cell type 2 and type 17 [corrected] responses. Am J Respir Crit Care Med 2009; 179:883-93.

Table S1

Name	Oligonucleotide Primer
Irf7	Forward: 5'-CTTAGCCGGGAGCTTGGATCTACT-3' Reverse: 5'-CCCTTGTACATGATGGTCACATCC-3'
Stat1	Forward: 5'-ACAGTGGTTCGAGCTTCAG-3' Reverse: 5'-GGCCAGGTACTGTCTGATTT-3'
Viperin	Forward: 5'- CGAAGACATGAATGAACACATCAA-3' Reverse: 5'-AATTAGGAGGCACTGGAAAACCT-3'
Hprt	Forward: 5'- AGGCCAGACTTTGTTGGATTTGAA-3' Reverse: 5'-CAACTTGCGCTCATCTTAGGCTTT-3'

Figure E1

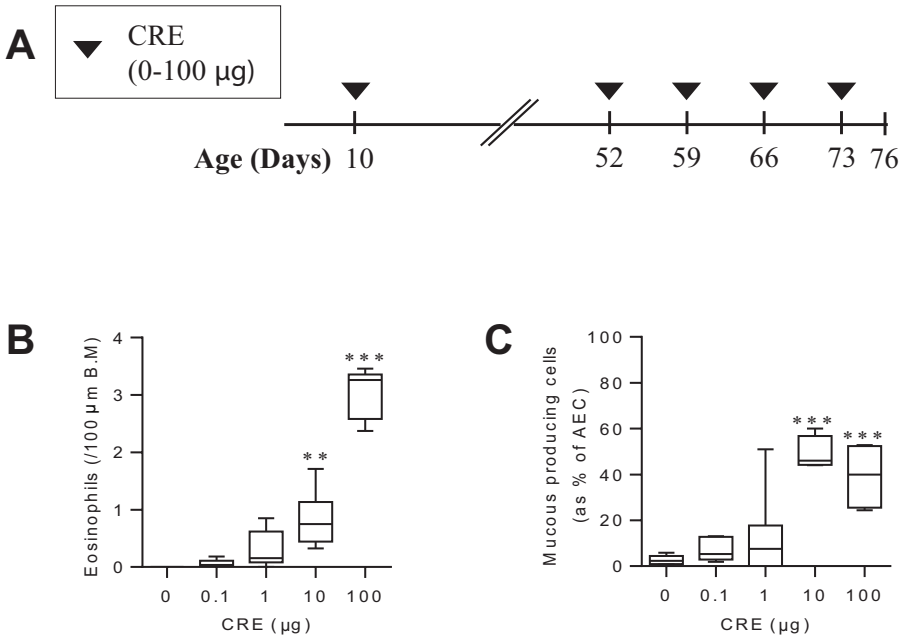
A
CRE
(0-100 µg)
Age (Days) 10
52
59
66
73
76
B
Eosinophils (/100 µm B.M)
0
1
2
3
4
**
***
0
0.1
1
10
100
CRE (µg)
C
Mucous producing cells
(as % of AEC)
0
20
40
60
80
100
***
***
0
0.1
1
10
100
CRE (µg)

Figure E2

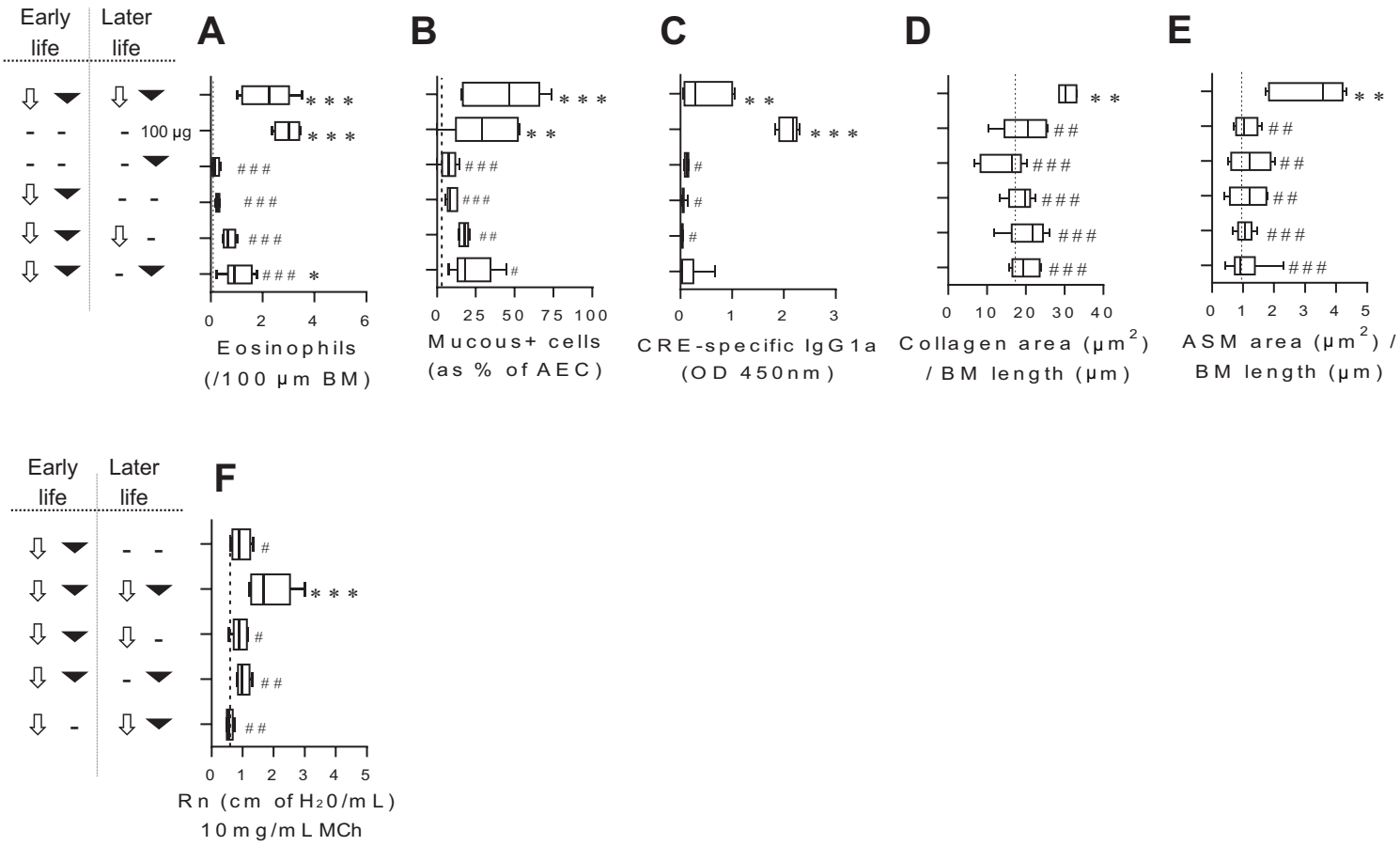
Early life
Later life
A
100 µg
Eosinophils (/100 µm BM)
B
Mucous+ cells (as % of AEC)
C
CRE-specific IgG1a (OD 450nm)
D
Collagen area (µm²) / BM length (µm)
E
ASM area (µm²) / BM length (µm)
F
Rn (cm of H20/mL) 10mg/mL MCh
G

Figure E3

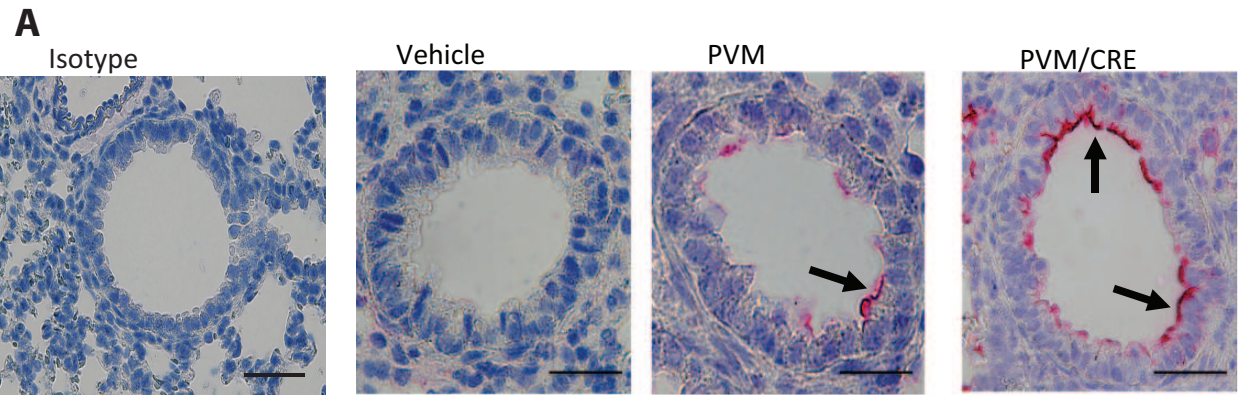
A
Isotype
Vehicle
PVM
PVM/CRE

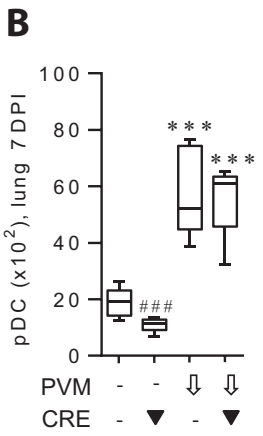
B
pDC (x10^2), lung 7DPI
PVM
CRE

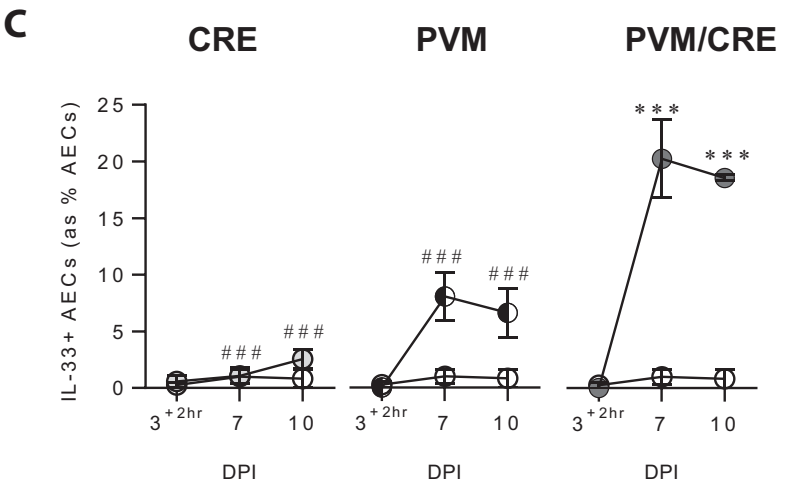
C
CRE
PVM
PVM/CRE
IL-33+ AECs (as % AECs)
DPI

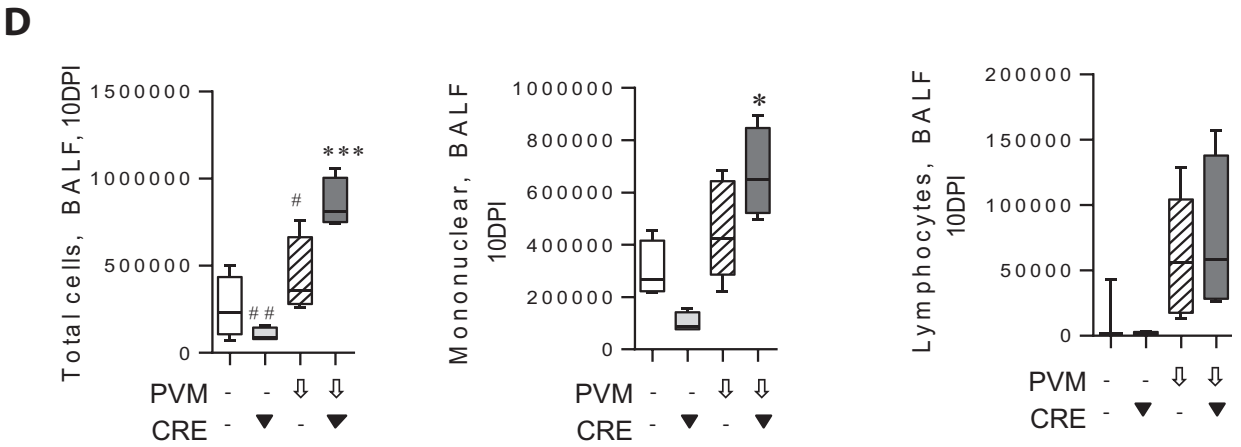
D
Total cells, BALF, 10DPI
Mononuclear, BALF 10DPI
Lymphocytes, BALF 10DPI
PVM
CRE

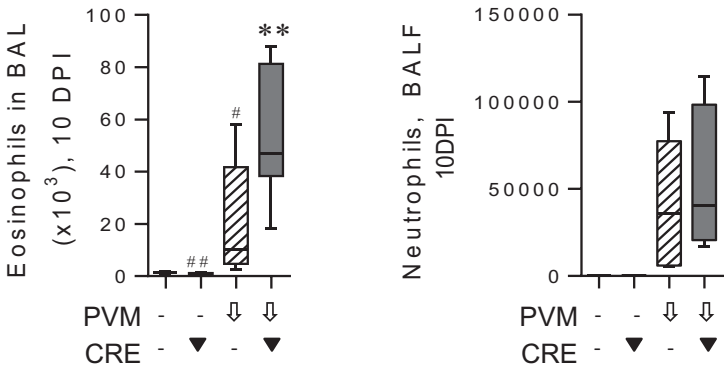
Eosinophils in BAL (x10^3), 10 DPI
Neutrophils, BALF 10DPI
PVM
CRE

Figure E4

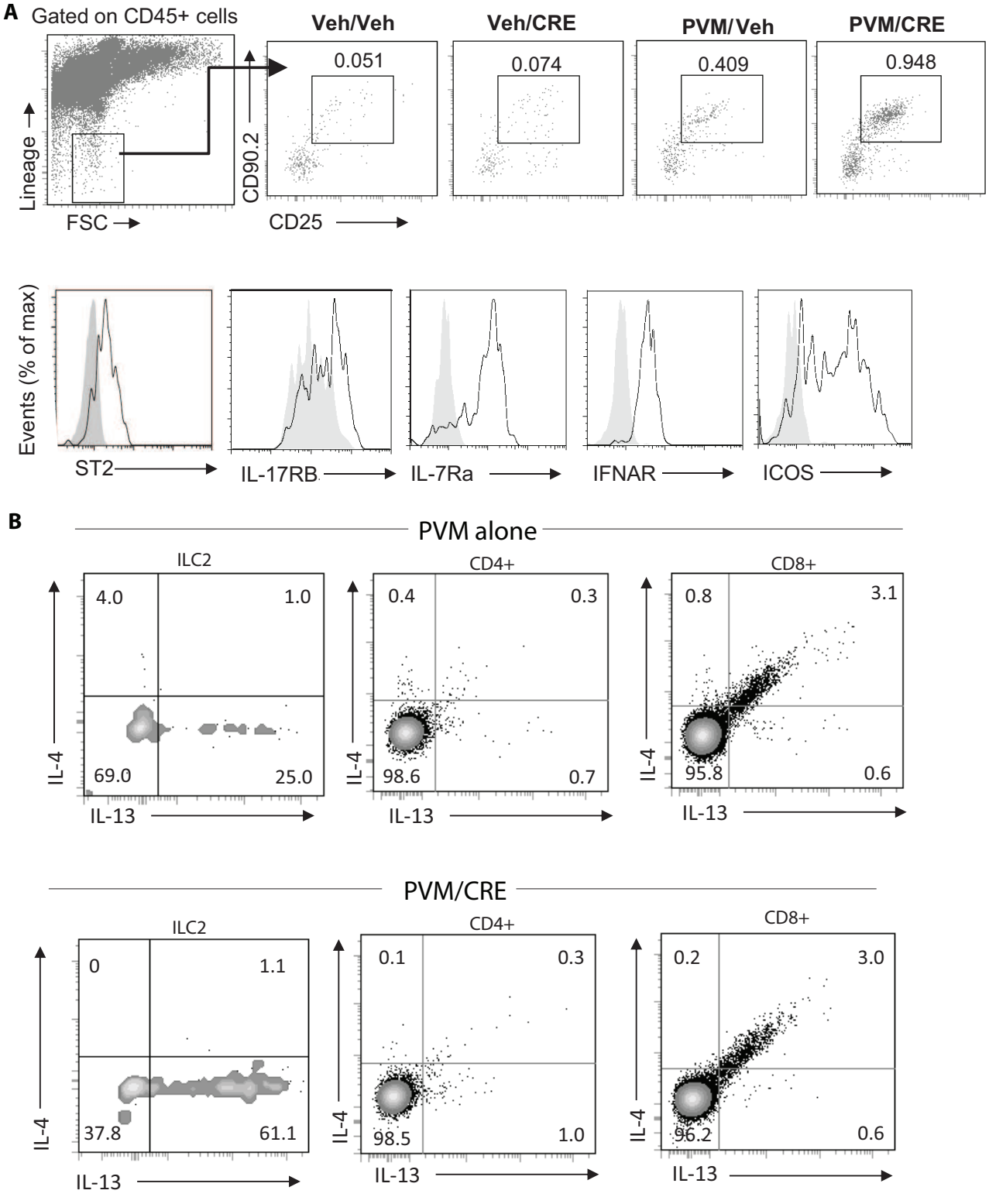
A
Gated on CD45+ cells
Veh/Veh
Veh/CRE
PVM/Veh
PVM/CRE
0.051
0.074
0.409
0.948
Lineage
FSC
CD90.2
CD25
Events (% of max)
ST2
IL-17RB
IL-7Ra
IFNAR
ICOS
B
PVM alone
ILC2
CD4+
CD8+
4.0
1.0
69.0
25.0
0.4
0.3
98.6
0.7
0.8
3.1
95.8
0.6
IL-4
IL-13
PVM/CRE
ILC2
CD4+
CD8+
0
1.1
37.8
61.1
0.1
0.3
98.5
1.0
0.2
3.0
96.2
0.6

Figure E5

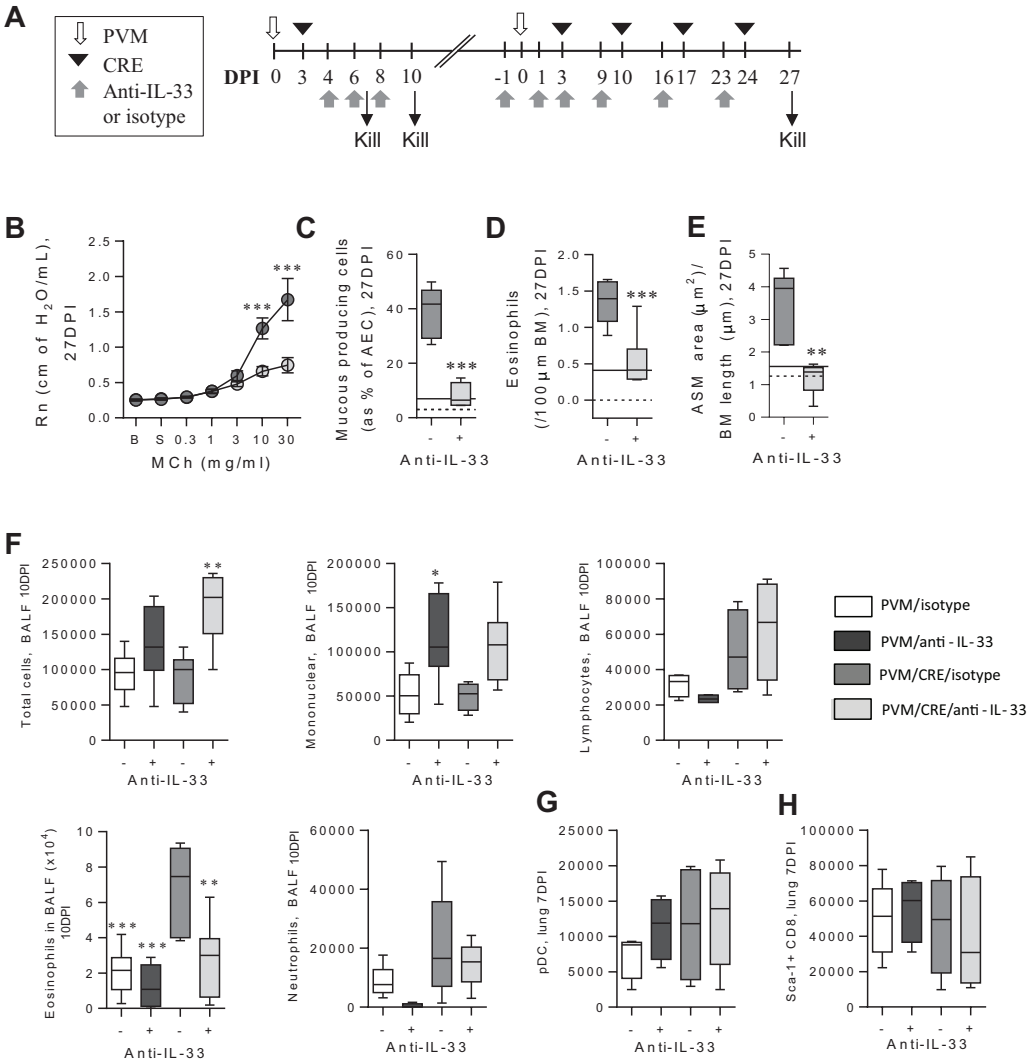
A
PVM
CRE
Anti-IL-33 or isotype
DPI 0 3 4 6 8 10 -1 0 1 3 9 10 16 17 23 24 27
Kill Kill Kill
B
Rn (cm of H2O/mL), 27DPI
MCh (mg/ml)
C
Mucous producing cells (as % of AEC), 27DPI
Anti-IL-33
D
Eosinophils (/100µm BM), 27DPI
Anti-IL-33
E
ASM area (µm2)/ BM length (µm), 27DPI
Anti-IL-33
F
Total cells, BALF 10DPI
Mononuclear, BALF 10DPI
Lymphocytes, BALF 10DPI
Eosinophils in BALF (x10^4) 10DPI
Neutrophils, BALF 10DPI
Anti-IL-33
PVM/isotype
PVM/anti-IL-33
PVM/CRE/isotype
PVM/CRE/anti-IL-33
G
pDC, lung 7DPI
H
Sca-1+ CD8, lung 7DPI

Figure E6

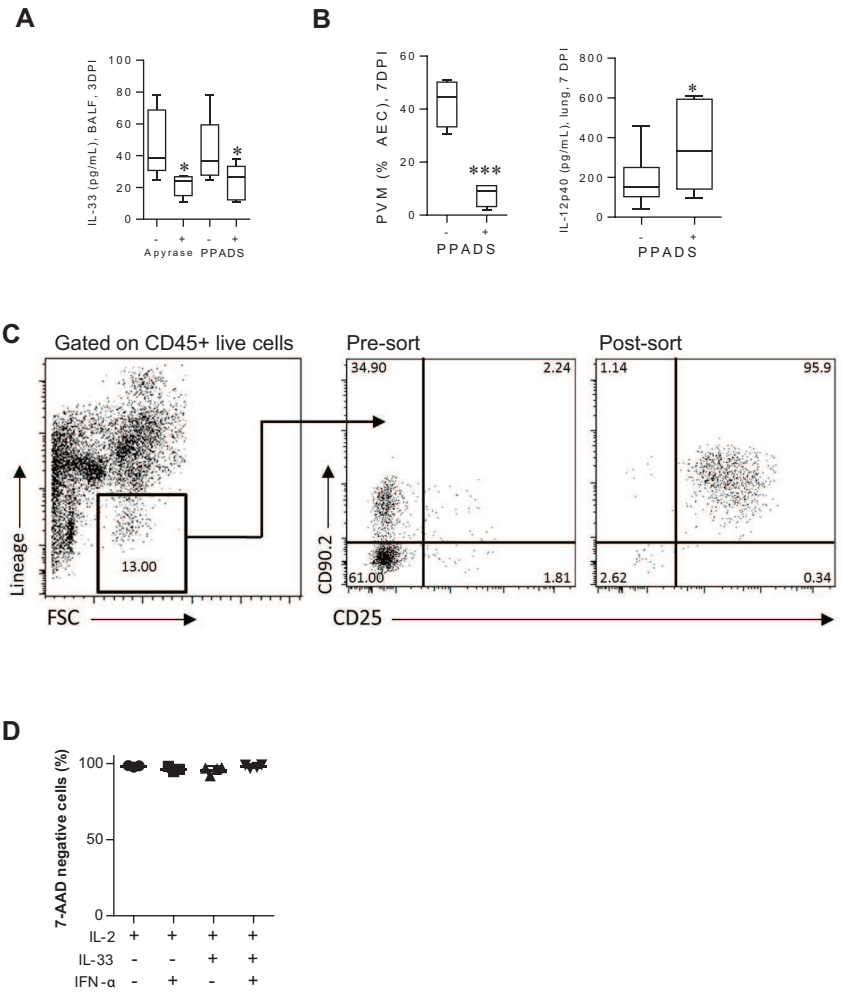
A
IL-33 (pg/mL), BALF, 3DPI
Apyrase
PPADS
B
PVM (% AEC), 7DPI
PPADS
IL-12p40 (pg/mL), lung, 7 DPI
PPADS
C
Gated on CD45+ live cells
Pre-sort
Post-sort
Lineage
FSC
13.00
CD90.2
CD25
34.90
2.24
61.00
1.81
1.14
95.9
2.62
0.34
D
7-AAD negative cells (%)
IL-2
IL-33
IFN-α

Figure E7

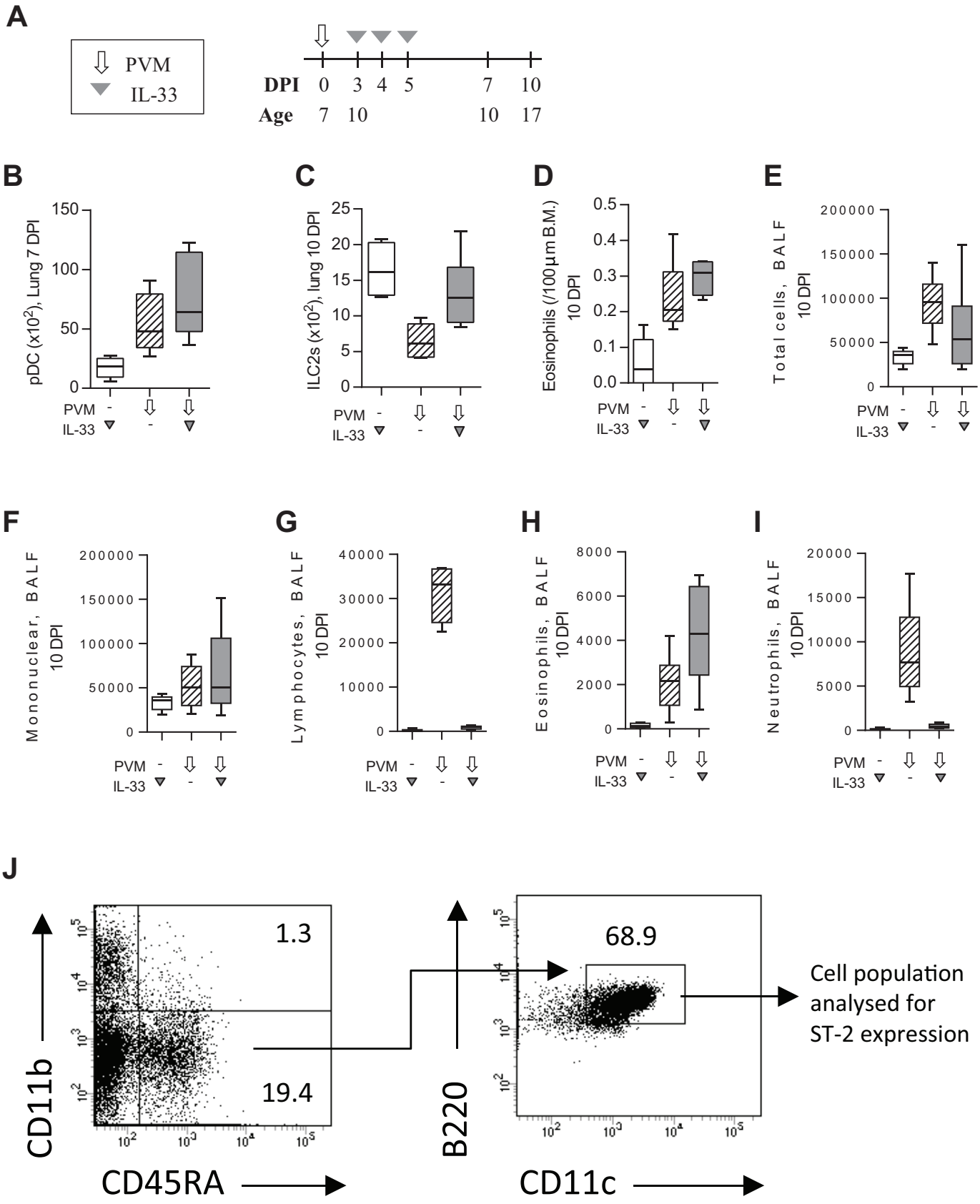
A
PVM
IL-33
DPI 0 3 4 5 7 10
Age 7 10 10 17
B
pDC (x10²), Lung 7 DPI
C
ILC2s (x10²), lung 10 DPI
D
Eosinophils (/100µm B.M.) 10 DPI
E
Total cells, BALF 10 DPI
F
Mononuclear, BALF 10 DPI
G
Lymphocytes, BALF 10 DPI
H
Eosinophils, BALF 10 DPI
I
Neutrophils, BALF 10 DPI
J
1.3
19.4
68.9
CD11b
CD45RA
B220
CD11c
Cell population analysed for ST-2 expression